JOURNAL OF GEOPHYSICAL RESEARCH, VOL. 115, D03107, doi:10.1029/2009JD012530, 2010

Analyses and development of a hierarchy of frozen soil models for cold region study

Qian Li,[1] Shufen Sun,[2] and Yongkang Xue[3]

Received 22 May 2009; revised 2 October 2009; accepted 12 October 2009; published 3 February 2010.

[1] Numerous frozen soil models currently in use differ in the complexity of their governing equations or/and in the processes being considered. It is important to comprehensively examine and categorize these on the basis of physical principles, assumptions, and relationship to each other. In this paper frozen soil models are classified into different levels according to the complexity of the governing equations. On the basis of scale analysis, models with different levels of complexity were derived from the most complicated frozen soil model. Rationales for the simplification of models at different levels are discussed. To overcome the difficulties in achieving numerical solutions, a new method of substituting soil enthalpy and total water mass for soil temperature and volumetric liquid water content in governing equations is introduced for each level of the frozen soil models. Models with different complexity levels are assessed with observational data. The preliminary monthly and seasonal evaluation shows that the results from the models with different complexity are generally similar but with substantial differences at the Tibetan D66 site during the melting and freezing period. The model including the contribution of vapor flux due to the matric potential gradient to the water balance performs the best at the D66 site. Compared to the corresponding original models, the frozen soil model versions with enthalpy and total water mass for governing equations appear to produce consistently better performance. Furthermore, the rationale of different methods for the freezing-melting process in frozen soil is discussed. It has been noted that the model derived from the freezing point depression equation and the soil matric potential equation is supported by both thermodynamic equilibrium theory and the simulation results.

Citation: Li, Q., S. Sun, and Y. Xue (2010), Analyses and development of a hierarchy of frozen soil models for cold region study, *J. Geophys. Res.*, *115*, D03107, doi:10.1029/2009JD012530.

1. Introduction

[2] Regions with frozen ground cover approximately 55%–60% of the exposed land surface in the Northern Hemisphere [*Zhang et al.*, 1999]. The coexistence of ice and liquid water changes the hydraulic and thermal properties of soil [*Jame and Norum*, 1980; *Cherkauer and Lettenmaier*, 1999], which in turn alters the distribution of water and energy in soil and their exchange with the overlying atmosphere. Frozen ground processes produce great effects on global and regional climate and hydrology [e.g., *Viterbo et al.*, 1999; *Poutou et al.*, 2004]. Furthermore, cryogenic soil can release abundant CO_2 and CH_4 when it thaws [e.g., *Zimov et al.*, 1993; *Elberling and Brandt*, 2003], which is considered a positive climate feedback and will be important to global climate change in the context of global warming [*Cox et al.*, 2000; *Friedlingstein et al.*, 2001]. Therefore, it is necessary to introduce frozen soil processes into land surface modeling and investigate their impact on climate, hydrology, and the carbon cycle.

[3] The development of frozen soil models, which included coupled heat and mass transport processes, began in the 1970s. After the International Geophysical Year, studies [e.g., *Ferrians et al.*, 1969; *Williams*, 1970] indicated that many engineering and hydrology problems were associated with soil freezing and thawing in cold regions. In addition, the introduction of computers during the 1970s also helped the development of numerical models that were specifically designed to solve the heat and water balance equations in frozen ground [*Cary and Mayland*, 1972; *Harlan*, 1973; *Guymon and Luthin*, 1974; *Taylor and Luthin*, 1978; *Fuchs et al.*, 1978]. In earlier studies, vapor fluxes and their phase changes were neglected for simplicity [*Cary and Mayland*, 1972; *Harlan*, 1973; *Guymon and Luthin*, 1974; *Fuchs et al.*, 1978]. Because more evidence has revealed the complexity of frozen soil processes and

[1]Center for Monsoon System Research, Institute of Atmospheric Physics, Chinese Academy of Sciences, Beijing, China.
[2]State Key Laboratory of Numerical Modeling for Atmospheric Sciences and Geophysical Fluid Dynamics, Institute of Atmospheric Physics, Chinese Academy of Sciences, Beijing, China.
[3]Department of Geography, Department of Atmospheric and Oceanic Sciences, University of California, Los Angeles, California, USA.

0148-0227/10/2009JD012530$09.00

their importance in climate models, sophisticated models have emerged during the past decade [e.g., *Flerchinger and Saxton*, 1989; *Zhao et al.*, 1997; *Jordan*, 1991]. Thus far, a large variety of frozen soil models or parameterizations with different levels of complexity have been developed. Their development has laid a good foundation for the synthesis of these frozen soil models and for delineating challenging issues in frozen soil modeling.

[4] Current frozen soil models are quite different in their governing equations in terms of prognostic and diagnostic variables. The most comprehensive as well as complicated frozen soil model [*Jordan*, 1991; *Zhao et al.*, 1997] includes four prognostic equations and five diagnostic equations together with one assumption to determine 10 variables. The relatively simple models, which are currently used the most often, only include two prognostic equations for temperature and liquid water content. Furthermore, these models also differ in their complexity of physical processes. For example, some take into account the contribution of vapor movement and its phase change in the water and heat balances [e.g., *Flerchinger and Saxton*, 1989; *Jansson and Karlberg*, 2001], while others [e.g., *Engelmark and Svensson*, 1993; *Slater et al.*, 1998; *Cherkauer and Lettenmaier*, 1999] neglect these contributions assuming that they are insignificant in the frozen soil process. In addition, models differ in whether the heat due to liquid water flux in the heat balance equation is considered, with a few models including this consideration [e.g., *Cary and Mayland*, 1972; *Harlan*, 1973; *Guymon and Luthin*, 1974; *Fuchs et al.*, 1978; *Shoop and Bigl*, 1997; *Pauwels and Wood*, 1999].

[5] Accurate simulation of the thermal regime in frozen soil models plays an important role in the prediction of global climate changes [*Ling and Zhang*, 2004], and temperature variation can affect the performance of structures constructed in cold regions [*Esch and Osterkamp*, 1990; *Lunardini*, 1996]. A frozen soil model with realistic simulation of soil temperature, liquid water content, and ice content also improved the climate model's ability to simulate greenhouse gas exchange processes in cold regions [*Mikan et al.*, 2002]. Since there are numerous frozen soil models with different heat and water equations, it is important to comprehensively examine and categorize them on the basis of physical principles, philosophies, assumptions, and their relationship to each other. This should help us better understand frozen soil processes and application of these models in climate research. To our knowledge, this type of review has not been done. In this paper, we will also address the following questions: (1) Is there any relationship among these models? Or can a simple frozen soil model be derived from the more complex models? (2) Do these models have comparable or different accuracies in simulating the distribution and variation of soil liquid water content and soil temperature in frozen soil? This paper groups frozen soil models into different hierarchical levels based on the completeness and complexity of their governing equations and then discusses relevant issues. Scale analysis is applied to examine the justification for simplification of frozen soil models.

[6] In most currently popular frozen soil models, there are only two governing equations with three unknown variables (temperature, liquid water content, and ice content). To obtain the solution of these equations, another relationship is required, which is normally done by quantitatively defining a relationship between liquid water content, ice content, and temperature, an important aspect in frozen soil modeling. We call this aspect the freezing-melting process scheme in this paper. Although there are many different parameterizations dealing with this issue, a comprehensive analysis investigating the rationale behind these freezing-thawing process schemes and their impact on the frozen soil solution has not been carried out. Therefore, this paper will present analyses and numerical sensitivity studies to examine these freezing-melting schemes' rationales and compare their simulation results with observational data.

[7] Obtaining the proper numerical solution is another important aspect in frozen soil modeling. The most difficult part of this work is to deal with a common term of ice-liquid phase change rate, which involves a highly nonlinear relationship between ice content, soil temperature, and liquid water in frozen soil. Estimation of ice content in numerical iteration, a common approach to solving frozen soil equations, normally introduces great errors into temperature and soil liquid water calculations, because of large latent heat energy associated with the ice-liquid phase change. This causes either difficulty in obtaining the numerical solution or even a failure to reach convergence. A comprehensive discussion of numerical methods is outside the scope of this paper. We develop a new approach to avoiding the estimation of ice content in the iteration procedure. Within the introduced hierarchical framework in this paper, we develop a new set of governing equations for frozen soil models using the methodology of variable transformation in which enthalpy and total water mass are introduced. Theoretical analysis and numerical testing using observational data indicate that this approach, in conjunction with a new effective numerical procedure, is able to obtain proper numerical solutions without lengthy iterations and therefore is appropriate for global climate studies.

[8] In this paper, different frozen soil models with various complexities are categorized in section 2. Their justifications are also discussed. On the basis of these discussions, a new set of frozen soil schemes with enthalpy and total water mass for governing equations is introduced. Section 3 discusses different freezing-melting process schemes. Section 4 evaluates frozen soil models and frozen-melting process schemes with observational data. Section 5 summarizes the results. We reserve a more detailed derivation of scale analysis for the Appendixes A and B.

2. Hierarchy of Governing Equations of Frozen Soil Models with Different Complexities

2.1. Level 1 Model: Complicated Frozen Soil Model

[9] The most complicated frozen soil model is labeled as a level 1 model in this paper. The equations are briefly presented in this section and the explanations for each symbol and their units are listed in the notation section.

[10] The change in the volumetric content of ice θ_i is given by

$$\frac{\partial \theta_i}{\partial t} + \frac{\dot{M}_{i,v} + \dot{M}_{i,l}}{\rho_i} = 0, \tag{1}$$

where subscripts i, v, and l represent ice, vapor, and liquid water content, respectively, in this paper; $\dot{M}$ represents the moisture transfer rate between different phases, and ρ is density.

[11] The change in the volumetric content of water θ_l is given by

$$\frac{\partial \theta_l}{\partial t} + \frac{\partial u_l}{\partial z} + \frac{\dot{M}_{l,v} - \dot{M}_{i,l}}{\rho_l} = 0, \tag{2}$$

where u_l is the velocity of the liquid water flow.

[12] The change in the volumetric mass content of vapor is given by

$$\frac{\partial \theta_v \rho_v}{\partial t} - \dot{M}_{i,v} - \dot{M}_{l,v} = \frac{\partial}{\partial z}\left[D_{eff}\frac{\partial \rho_v}{\partial Z}\right], \tag{3}$$

where D_{eff} denotes the effective diffusivity. The energy equation to describe the change of temperature T is given by

$$\frac{\partial C_v T}{\partial t} - L_{i,l}\frac{\partial \rho_i \theta_i}{\partial t} + L_{l,v}\frac{\partial \rho_v \theta_v}{\partial t} = -\rho_l c_l \frac{\partial u_l T}{\partial Z} + L_{l,v}\frac{\partial}{\partial Z}\left(D_{eff}\frac{\partial \rho_v}{\partial Z}\right) + \frac{\partial}{\partial Z}\left(K_{eff}\frac{\partial T}{\partial Z}\right), \tag{4}$$

where L represents the latent heat from changes between different phases, C is the volumetric heat capacity, and K is the conductivity.

[13] The u_l is described by Darcy's law:

$$u_l = K_l\left[-\frac{\partial \psi}{\partial Z} + 1\right]. \tag{5}$$

[14] In unsaturated frozen soil, the constitutive relationship of the soil matric potential ψ should be a function of both liquid water and ice content if the osmotic potential is neglected [*Kulik*, 1978; *Koren et al.*, 1999],

$$\psi = \psi_0\left(\frac{\theta_l}{\theta_s}\right)^{-b}(1 + c_k\theta_i)^2, \tag{6}$$

where θ_l is the volumetric soil liquid water content and θ_s is the volumetric soil liquid water content at saturation. The ρ_v is related to local equilibrium vapor pressure e_v in soil,

$$\rho_v = \frac{e_v}{R_v T}. \tag{7}$$

On the basis of the derivation using thermodynamic equilibrium theory [*Williams*, 1967; *Zhang et al.*, 2007], the freezing point depression relation between maximum ψ and T for frozen soil should be

$$\psi = \frac{L_{i,l}(T - T_f)}{gT_f}\ (T < T_f), \tag{8}$$

where T_f is the freezing point of free water (273.15 K). The θ_v is given by

$$\theta_v = \theta_s - \theta_i - \theta_l. \tag{9}$$

[15] There are 10 unknown variables (θ_i, θ_l, θ_v, ρ_v, T, u_l, ψ, $\dot{M}_{i,v}$, $\dot{M}_{l,v}$, and $\dot{M}_{i,l}$) but only nine equations (1)–(9). In order to close the equations, *Jordan* [1991] and *Zhao et al.* [1997] separately proposed additional (but different) phase change relationships between ice, liquid, and vapor. However, these relationships are just assumptions without any validation; hence, their applicability is unclear. Equations (1)–(9) together with the unspecified assumption are categorized as the level 1 model.

[16] The level 1 model takes the coupling effect of mass and heat transport into consideration and includes a detailed description of mass balances of volumetric liquid water, ice, and vapor content. It also considers contributions of heat conduction, phase change, liquid flow, and vapor gas diffusion to the energy balance. The establishment of the level 1 model is based on several assumptions, and the most important one is the assumption that within the local averaging volume, all phases (soil particle, ice, liquid water, and the gas mixture of water vapor and dry air) are in thermal equilibrium [*Zhao et al.*, 1997]. It means that all prognostic and diagnostic variables in the model are valid under thermal equilibrium and, accordingly, equation (8).

2.2. Level 2 Model: Medium Complexity Frozen Soil Model

[17] Although the level 1 model is relatively complete, it requires adding one arguable or unproven phase-transfer relation to solve the model equations. One way to overcome this problem is to simplify the governing equations in the level 1 model. It is clear that equation (5) is absolutely necessarily retained because water flow in soil (unfrozen or frozen) is assumed to be laminar and, thus, obeys Darcy's law as generalized for unsaturated flow by *Richards* [1931]. And the constitutive relationship of the soil matric potential, described as (6) in the level 1 model, is the important hydrologic relationship in soil physics that cannot be omitted. Equation (8) is based on thermodynamic equilibrium theory, which the model system must strictly obey.

[18] The simplification of the level 1 model, therefore, has to be conducted through the mass and heat balance equations of the level 1 model. Scale analysis of terms in these equations is employed in this paper (see Appendix A for detail). It has been found that the change in the volumetric mass content of vapor $\left(\frac{\partial \theta_v \rho_v}{\partial t}\right)$ is about two orders of magnitude less than that of vapor diffusion $\left(\frac{\partial}{\partial z}\left[D_{eff}\frac{\partial \rho_v}{\partial Z}\right]\right)$ in equation (3). Thus, after neglecting the term $\left(\frac{\partial \theta_v \rho_v}{\partial t}\right)$, which is 2 orders of magnitude smaller, equation (3) could be reduced to

$$\left(\dot{M}_{i,v} + \dot{M}_{l,v}\right) + \frac{\partial}{\partial Z}\left(D_{eff}\frac{\partial \rho_v}{\partial Z}\right) = 0. \tag{10}$$

After expanding the term of $\frac{\partial}{\partial Z}\left(D_{eff}\frac{\partial \rho_v}{\partial Z}\right)$ using equation (7) and making some mathematical manipulations [*Zhang*,

2004], equations (1), (2), (5), and (10) can be combined into the following:

$$\frac{\partial \theta_l}{\partial t} = -\frac{\rho_i}{\rho_l}\frac{\partial \theta_i}{\partial t} - \frac{\partial}{\partial Z}\left(-K_l\frac{\partial \psi}{\partial Z} + K_l\right) + \frac{1}{\rho_l}\frac{\partial}{\partial Z}\left(D_{TV}\frac{\partial T}{\partial Z} + D_{\psi V}\frac{\partial \psi}{\partial Z}\right). \quad (11)$$

In (11), the terms associated with moisture transfer between different phases have been eliminated. Similarly, after eliminating $\left(\frac{\partial \theta_v \rho_v}{\partial t}\right)$ and using equation (7), the energy equation (4) will become

$$\frac{\partial C_v T}{\partial t} - L_{i,l}\frac{\partial \rho_i \theta_i}{\partial t} = -\rho_l c_l \frac{\partial u_l T}{\partial Z} + L_{l,v}\frac{\partial}{\partial Z}\left(D_{TV}\frac{\partial T}{\partial Z} + D_{\psi V}\frac{\partial \psi}{\partial Z}\right) + \frac{\partial}{\partial Z}\left(K_{eff}\frac{\partial T}{\partial Z}\right). \quad (12)$$

Equations (11) and (12) together with (5), (6), and (8) are categorized as the level 2 model, which simplifies the level 1 model because it only consists of five equations for five unknown variables (θ_i, θ_l, T, u_l, ψ). It does not require the information of $\dot{M}_{i,v}$, $\dot{M}_{l,v}$, and $\dot{M}_{i,l}$ and does not require any additional assumptions. The level 2 model still takes the coupling effect of mass and heat transport into consideration just as the level 1 model does. The original derivation of this type of model is based on the principles of the linear thermodynamics of irreversible processes and includes cross-effects such as the Ludwig-Soret effect and Dufour effect [*Mölders and Walsh*, 2004].

2.3. Level 3 Model and Level 4 Model

[19] The level 2 model is simpler than the level 1 model with regard to the number of equations and unknown variables, but it is still too complex for climate studies. Therefore, many simple frozen soil models have been developed for frozen soil process studies. Currently the most widely used frozen soil models are simplified versions of level 2 with simplifications in different terms of the level 2 equations. For instance, the earlier models proposed by *Harlan* [1973], *Guymon and Luthin* [1974], and *Fuchs et al.* [1978] neglected the third term on the right-hand side of equation (11), which represents the contribution of vapor fluxes to the mass balance, and the second term on the right-hand side of equation (12), which represents the contribution of the heat flux by vapor phase change to the energy balance. *Guymon and Luthin* [1974] pointed out that the assumption that vapor flux has negligible effects on water transfer is valid for moist soils. *Fuchs et al.* [1978] calculated the contribution of the vapor phase to heat transfer and also showed that it was insignificant. In addition, some models neglected the first term on the right-hand side of equation (12), which corresponds to the heat flux term due to liquid flow [*Engelmark and Svensson*, 1993; *Slater et al.*, 1998; *Cherkauer and Lettenmaier*, 1999].

[20] In view of the fact that there are various models with different simplifications and they are all widely used in current frozen soil studies, the justifications for these simplifications and an examination of their accuracy are essential for land surface model development. Through this process, it is possible to expose the simplest model which has reasonable accuracy. In this section, we continue carrying out scale analysis to evaluate the order of magnitude of each term in the level 2 model equations and to further simplify them. Evaluation of the magnitude of flux terms in the energy and mass balance equations is conducted under a wide range of soil temperature, soil texture, and ice content for six typical soil textures (sand, sandy loam, loam, silt loam, sandy clay, and clay). The values of every term related to heat and water fluxes in the equations of the level 2 model category for six soil textures under different conditions have been calculated and analyzed (see Appendix B).

[21] According to the results in Appendix B, for energy balance, the second term on the right-hand side of equation (12), $L_{l,v}\frac{\partial q_v}{\partial Z}$, which represents heat flux by vapor phase, is very small compared to the third term representing heat conduction flux on the right-hand side of equation (12) and can be neglected. Even the term for heat flux by liquid flow (the first term on the right-hand side of equation (12)) is also very small within soil when compared with heat conduction and can also be neglected. Only at the soil surface layer is the heat flux term for infiltrating water comparable to the heat conduction term. According to the above analysis, the heat balance equation based on (12) can be simplified to

$$\frac{\partial C_v T}{\partial t} - L_{i,l}\frac{\partial \rho_i \theta_i}{\partial t} = \frac{\partial}{\partial Z}\left(K_{eff}\frac{\partial T}{\partial Z}\right). \quad (13)$$

[22] In this paper, equations (11) and (13) together with (6) and (8) are referred to as the level 3 model [e.g., *Zhang et al.*, 2007]. It consists of four equations for four unknown variables (θ_i,θ_l, T, and ψ).

[23] For the mass balance equation, the third term on the right-hand side of equation (11), $\frac{+\partial q_v}{\rho_l \partial Z}$, which corresponds to the vapor flux, only shows a small contribution when compared with the moisture flux under most cases and, therefore, can be neglected as done in many frozen soil schemes [*Harlan*, 1973; *Guymon and Luthin*, 1974; *Fuchs et al.*, 1978; *Engelmark and Svensson*, 1993; *Shoop and Bigl*, 1997; *Slater et al.*, 1998; *Cherkauer and Lettenmaier*, 1999; *Koren et al.*, 1999; *Pauwels and Wood*, 1999]. After this simplification, the water balance equation can be written as

$$\frac{\partial \theta_l}{\partial t} = -\frac{\rho_i}{\rho_l}\frac{\partial \theta_i}{\partial t} - \frac{\partial}{\partial Z}\left(-K_l\frac{\partial \psi}{\partial Z} + K_l\right). \quad (14)$$

Equations (14) and (13) together with (6) and (8) are referred to as the level 4 model.

[24] The level 3 model is a mixture of the level 2 and level 4 models because it has the same water balance equation as in level 2 and the same energy balance equation as in level 4. When soil is relatively dry, the moisture flux term becomes small and the vapor flux components can be comparable to the moisture flux term, although under normal conditions it is small. In order to make the model suitable for various soils at a wide range of soil temperature and wetness, it is desirable to retain the water balance

Table 1. Primary Equations for Models at Different Levels and References[a]

Model	Water Balance Equation	Energy Balance Equation
Level 1	$\frac{\partial\theta_l}{\partial t} = -\frac{\rho_i}{\rho_l}\frac{\partial\theta_i}{\partial t} - \frac{\partial}{\partial Z}\left(-K_l\frac{\partial\psi}{\partial Z} + K_l\right) - \frac{1}{\rho_l}\left(\frac{\partial\theta_v\rho_v}{\partial t} - \frac{\partial q_v}{\partial z}\right)$ *Jordan* [1991] (SNTHERM); *Zhao et al.* [1997]	$\frac{\partial C_v T}{\partial t} - L_{il}\frac{\partial\rho_i\theta_i}{\partial t} = -\rho_l c_l\frac{\partial u_l T}{\partial Z} + L_{lv}\left(\frac{\partial\theta_v\rho_v}{\partial t} + \frac{\partial q_v}{\partial z}\right) + \frac{\partial}{\partial Z}\left(K_{\mathrm{eff}}\frac{\partial T}{\partial Z}\right)$ *Flerchinger and Saxton* [1989]; *Jordan* [1991] (SNTHERM); *Zhao et al.* [1997]
Level 2	$\frac{\partial\theta_l}{\partial t} = -\frac{\rho_i}{\rho_l}\frac{\partial\theta_i}{\partial t} - \frac{\partial}{\partial Z}\left(-K_l\frac{\partial\psi}{\partial Z} + K_l\right) + \frac{1}{\rho_l}\frac{\partial q_v}{\partial Z}$ *Flerchinger and Saxton* [1989]; *Jansson and Karlberg* [2001] (COUP) *Zhang et al.* [2007]	$\frac{\partial C_v T}{\partial t} - L_{il}\frac{\partial\rho_i\theta_i}{\partial t} = -\rho_l c_l\frac{\partial u_l T}{\partial Z} + L_{lv}\frac{\partial q_v}{\partial z} + \frac{\partial}{\partial Z}\left(K_{\mathrm{eff}}\frac{\partial T}{\partial Z}\right)$ *Jansson and Karlberg* [2001] (COUP)
Level 2.5	$\frac{\partial m_a}{\partial t} = -\rho_l\frac{\partial}{\partial Z}\left(-K_l\frac{\partial\psi}{\partial Z} + K_l\right) + \frac{\partial q_v}{\partial Z}$ *Li* [2008]	$\frac{\partial H}{\partial t} = \frac{\partial}{\partial Z}\left(K_{\mathrm{eff}}\frac{\partial T}{\partial Z}\right) - \rho_l c_l\frac{\partial u_l T}{\partial Z} + L_{l,v}\frac{\partial q_v}{\partial Z}$ *Li* [2008]
Level 3	$\frac{\partial\theta_l}{\partial t} = -\frac{\rho_i}{\rho_l}\frac{\partial\theta_i}{\partial t} - \frac{\partial}{\partial Z}\left(-K_l\frac{\partial\psi}{\partial Z} + K_l\right) + \frac{1}{\rho_l}\frac{\partial q_v}{\partial Z}$ *Flerchinger and Saxton* [1989]; *Zhang et al.* [2007]	$\frac{\partial C_v T}{\partial t} - L_{il}\frac{\partial\rho_i\theta_i}{\partial t} = \frac{\partial}{\partial Z}\left(K_{\mathrm{eff}}\frac{\partial T}{\partial Z}\right)$ *Jame and Norum* [1980]; *Engelmark and Svensson* [1993]; *Romanovsky et al.* [1997]; *Slater and Pitman* [1998] (BASE); *Koren et al.* [1999] (LSM); *Cherkauer and Lettenmaier* [1999]; *Takata and Kimoto* [2000]; *Smirnova et al.* [2000] (MAPS); *Warrach et al.* [2001] (SEWAB); *Ling and Zhang* [2004]; *Niu and Yang* [2006] (CLM2.0); *Zhang et al.* [2007]
Level 3.5	$\frac{\partial m_a}{\partial t} = -\rho_l\frac{\partial}{\partial Z}\left(-K_l\frac{\partial\psi}{\partial Z} + K_l\right) + \frac{\partial q_v}{\partial Z}$ *Li* [2008]	$\frac{\partial H}{\partial t} = \frac{\partial}{\partial Z}\left(K_{\mathrm{eff}}\frac{\partial T}{\partial Z}\right)$ *Li* [2008]
Level 4	$\frac{\partial\theta_l}{\partial t} = -\frac{\rho_i}{\rho_l}\frac{\partial\theta_i}{\partial t} - \frac{\partial}{\partial Z}\left(-K_l\frac{\partial\psi}{\partial Z} + K_l\right)$ *Cary and Mayland* [1972]; *Harlan* [1973]; *Guymon and Luthin* [1974]; *Fuchs* [1978]; *Jame and Norum* [1980]; *Shoop and Bigl* [1997] (FROSTB); *Slater and Pitman* [1998] (BASE); *Pauwels and Wood* [1999]; *Cherkauer and Lettenmaier* [1999]; *Cox et al.* [2000]	$\frac{\partial C_v T}{\partial t} - L_{il}\frac{\partial\rho_i\theta_i}{\partial t} = \frac{\partial}{\partial Z}\left(K_{\mathrm{eff}}\frac{\partial T}{\partial Z}\right)$ Same as references in the level 3 model
Level 4.5	$\frac{\partial m_a}{\partial t} = -\rho_l\frac{\partial}{\partial Z}\left(-K_l\frac{\partial\psi}{\partial Z} + K_l\right)$ *Li* [2008]	$\frac{\partial H}{\partial t} = \frac{\partial}{\partial Z}\left(K_{eff}\frac{\partial T}{\partial Z}\right)$ *Li* [2008]

[a]In the table, $\frac{\partial q_v}{\partial Z}$ means vapor flux and is equal to $\frac{\partial}{\partial Z}\left(D_{\mathrm{TV}}\frac{\partial T}{\partial Z} + D_{\psi\mathrm{V}}\frac{\partial\psi}{\partial Z}\right)$ in the paper.

equation as equation (11). This issue will be further discussed in section 4.

2.4. Transformation of Model Prognostic Variables

[25] In the different level models discussed above, temperature, ice, and liquid water content are applied in the prognostic equations. As indicated in section 1, iteration procedures are generally required to solve the highly nonlinear mass and energy balance equations in these models [*Celia et al.*, 1990; *Hansson et al.*, 2004; *Zhang et al.*, 2007], which requires an estimate of the ice content in the iteration procure. The estimation error in the ice content could cause large errors in the temperature calculation or make the solution difficult to obtain.

[26] In order to overcome this difficulty and avoid tuning parameters, which may achieve iteration convergence but results in parameters that vary by geographical area, the methodology of variable transformation is applied to level 2, level 3, and level 4 models, which leads to new schemes referred to as level 2.5, level 3.5, and level 4.5, respectively, in this paper. The new variables of enthalpy H ($H = C_v T - L_{i,l}\rho_i\theta_i$) and total water mass m_a ($m_a = \rho_i\theta_i + \rho_l\theta_l$) rather than the temperature and separate soil liquid water and ice content are used as the prognostic variables in the governing equations. Here we only show the new scheme for the level 3 model. The governing equations of level 2.5 and level 4.5 models are listed in Table 1. On the basis of level 3, we obtain

$$\frac{\partial m_a}{\partial t} = -\rho_l\frac{\partial}{\partial Z}\left(-K_l\frac{\partial\psi}{\partial Z} + K_l\right) + \frac{\partial}{\partial Z}\left(D_{\mathrm{TV}}\frac{\partial T}{\partial Z} + D_{\psi\mathrm{V}}\frac{\partial\psi}{\partial Z}\right), \tag{15}$$

$$\frac{\partial H}{\partial t} = \frac{\partial}{\partial Z}\left(K_{\mathrm{eff}}\frac{\partial T}{\partial Z}\right). \tag{16}$$

Equations (15) and (16) together with (6) and (8) are referred to as the level 3.5 model.

2.5. Summary of Models at Different Levels

[27] Table 1 lists the water and energy balance equations for different level models and some references. The models at every level take the soil temperature and liquid water content as prognostic variables and are only differentiated

by certain processes being considered or disregarded in the governing equations. In the governing equations of level 2.5, level 3.5, and level 4.5 models, the term for the ice-liquid phase change rate ($\frac{\partial \theta_i}{\partial t}$) which is explicitly used in level 1 through level 4 models, has been incorporated into the new prognostic variables H and m_a. A more efficient numerical scheme for those models has been designed [*Li*, 2008].

3. Different Methods for Dealing With the Freezing-Melting Process

[28] As indicated in section 1, there are two prognostic governing equations but three unknown variables (liquid water content θ_l, ice content θ_i, and temperature T) in most currently popular frozen soil models. It is necessary to introduce a freezing-melting process scheme in the frozen soil parameterization that quantitatively defines the relation between θ_l, θ_i, and T. In this section, we present four commonly used schemes in frozen soil modeling, and the impact of these different schemes on simulation results will be discussed in section 4.3.

[29] In the early development of land surface modeling, the freezing-melting process was considered as occurring at T_f (= 273.15 K) [e.g., *Sellers et al.*, 1986; *Xue et al.*, 1996]. Because of its simplicity and convenience in calculating three unknown variables in the frozen soil model, it has had wide application [e.g., *Slater et al.*, 1998, *Takata and Kimoto*, 2000; *Dai et al.*, 2003]. Because of its oversimplicity, *Dickinson et al.* [1993] considered the freezing-melting process to occur in a range between T_f and some temperature below T_f. The above two methods are based on some empirical evidence and are referred to as method 1 and method 2 in this paper.

[30] When more data are available, different empirical functions regarding temperature and unfrozen liquid water content or ice content are proposed on the basis of these data for different soil textures [*Pauwels and Wood*, 1999; *Xu et al.*, 2001; *Decker and Zeng*, 2006], and this is referred to as method 3 here. In this method, unfrozen soil water coexists with ice when soil temperature is much below T_f, which is in accord with observations.

[31] Another method, referred to as method 4, has recently been developed on the basis of the freezing-point depression equation (such as equation (8) in this paper). Since this equation employs the matric potential, a soil matric potential equation (such as equation (6)) that defines the relation of the matric potential with volumetric liquid water and ice content is also introduced. This method has been widely applied for frozen soil research [e.g., *Cherkauer and Lettenmaier*, 1999; Cox et al. 2000; *Koren et al.*, 1999; *Smirnova et al.*, 2000; *Warrach et al.*, 2001; *Mölders and Walsh*, 2004; *Niu and Yang*, 2006] and is employed in this paper with level 1 through level 4 models. In this method, the freezing-melting process is deemed to be continuous with no fixed freezing point.

[32] A freezing-melting process equation can be derived from equations (8) and (6) based on method 4 [*Zhao and Gray*, 1997], i.e.,

$$\theta_l = \theta_s \cdot \left[\frac{L_{i,l} \cdot (T - T_f)}{g \psi_o T_f} (1 + c_k \theta_i)^{-2} \right]^{-1/b} \quad (T < T_f). \qquad (17)$$

[33] Equation (17) reveals three important facts. First, liquid water will always exist in unsaturated frozen soil no matter how low the soil temperature is; that is, there is no fixed point or range of freezing temperature where soil liquid water will be frozen completely. Second, assuming that the volumetric content of ice θ_i equals zero, the amount of θ_l calculated from equation (6) is the soil's capacity for holding liquid water that will not freeze at a temperature T below 0°C. It means that liquid water in soil with temperature T will freeze only when the volumetric liquid water content θ_l is greater than the holding capacity. Third, owing to different ψ_0 and θ_s for different soil textures, there are different maximum holding capacities of liquid water for different soil textures. All of these details are consistent with observations.

[34] Please note that the models from level 1 to level 4 using method 4, which includes equation (8), are closed; that is, the number of unknown variables is equal to the number of equations. Any new relationship (i.e., other than method 4) that is added to the models should be able to reasonably replace the freezing-point depression equation (equation (8)) and/or soil matric potential equation (equation (6)) or, at least, should be able to be derived from these two equations. We will discuss this further in section 4.3.

4. Testing Models and Freezing-Melting Process Schemes

[35] Since a comprehensive evaluation of frozen soil models is outside the scope of this paper, we only conducted preliminary tests for frozen soil models at the different levels with three observational data sets, in order to conduct some basic evaluations. The level 1 model is too complicated to be used in long-term climate simulations and is not evaluated in this paper.

[36] In the experiments, the surface fluxes and energy balance are calculated using the similar parameterizations as discussed by *Sun et al.* [1999] for every model. The models with different levels use the same hydraulic and thermal parameters, e.g., soil hydraulic conductivity and soil thermal conductivity. There are 17 layers in each frozen soil model. The thickness of the top soil layer is 2 cm and the bottom layer is set at a depth of 6 m. The top 60 cm soil layers are set with high vertical resolution, and the deep soil layers are set with coarse resolution. All soil parameters at different model levels are the same for each test site. As discussed earlier, models of different levels are different because of the terms included in the governing equations.

4.1. Field Data for Testing

[37] Three data sets from the GEWEX Asia Monsoon Experiment (GAME)/Tibet D66 site, the Tibet D105 site, and the Rosemount Station from the University of Minnesota are used to evaluate level 2 through level 4.5 model performance and to assess freezing-melting process schemes.

4.1.1. GAME/Tibet D66 Data

[38] The D66 site is located in the northern part of the Tibetan Plateau (35°31′N, 93°47′E, 4560 m elevation). The soil at this site is in a permafrost state with inhomogeneous texture in the vertical direction, and its type is sandy loam.

The site is flat with unusually sparse grassland. Soil water content was measured hourly with time domain reflectometry (TDR) at six depths: 4, 20, 60, 100, 160, and 225 cm. Soil temperature was measured hourly with 10 platinum (Pt) ground temperature probes at 10 depths: 4, 20, 40, 60, 80, 100, 130, 160, 200, and 263 cm, with ground surface temperature measured by the Infrared Radiation Thermometer. An automatic weather station measured meteorological data including downward solar radiation flux, air temperature, pressure, relative humidity, and wind speed. The model simulation is performed for 1 October to 1 November 1997 when the soil was frozen but had no overlying snow cover.

4.1.2. Tibet D105 Data

[39] The D105 site (33.07°N, 91.94°E, 5020 m elevation) is located on the north slope of the Tanggula Mountains, near the 105 Management Station (Daoban) of the Qinghai-Xizang (Tibetan) Highway. It is in the permafrost region and the soil type is mostly silt. Soil temperature was measured hourly with Pt ground temperature probes at four depths: 4, 10, 20, and 40 cm. An automatic weather station measured meteorological data including downward solar radiation flux, upward shortwave radiation flux, downward and upward longwave radiation flux, air temperature, pressure, relative humidity, and wind speed. The model simulation is performed for the period from 1 November 2000 to 31 May 2001, when the soil experienced freezing and thawing.

4.1.3. Rosemount Field Experiment Data

[40] The Rosemount Station is located approximately 25 km south of Saint Paul, Minnesota (44°43′N, 93°05′W, 290 m elevation), and the site is in a relatively flat field. The soil at Rosemount is a Waukegan silt loam [*Spaans and Baker*, 1996]. The soil liquid water content and temperature were measured with an automated, multiplexed TDR system and precision-calibrated thermistors, respectively, at eight depths: 5, 10, 16, 20, 31, 48, 65, and 100 cm [*Baker and Allmaras*, 1990]. Available meteorological data, including incoming and reflected solar radiation, incoming and outgoing long-wave radiation, air temperature, relative humidity, barometric pressure, wind speed, and precipitation, were measured at a 30 min interval. Seasonal freezing occurs in winter and thawing occurs in spring.

4.2. Evaluation of Frozen Soil Models at Different Levels

[41] The D66 data, Rosemount data, and D105 data are used to drive different level models, and results are compared with those observations. The first two data sets last about 2 months when no snow cover exists; the D105 data set covers half a year. The results produced by different level models, especially level 2.5 and level 3.5, are generally in good agreement with observational data sets in both magnitude and variability. Figures 1 and 2 show the results obtained by using the level 3.5 model for the D66 site and the D105 site, respectively. For conciseness, we only show results from the level 3.5 model. The results from other levels are similar. It can be found that even while Figure 1 shows good performance of the level 3.5 model, the simulated soil temperature at 4 and 20 cm are lower than observation. This difference is probably induced by the improper thermal conductivity in the model. In fact, the vertical heterogeneity of soil texture at site D66 is obvious. When soil freezes the existence of soil ice changes the thermal conductivity greatly, which enhances the heterogeneity and the difficulty of parameterizing it. As for the difference of soil liquid water content between the simulation and observations, it can also be related to the vertical heterogeneity of hydraulic conductivity.

[42] To quantitatively assess the performance of these models, statistical analyses on results from level 2 through level 4.5 models are conducted. The root mean square error (RMSE), which is a measure of nonsystematic error, and the mean bias error (MBE), which provides a measure of systematic error [*Halliwell and Rouse*, 1989], are used to compare the performance of the models:

$$\mathrm{RMSE} = \sqrt{\frac{\sum_{i=1}^{N} [P_\mathrm{i} - O_\mathrm{i}]^2}{N}} \qquad \mathrm{MBE} = \frac{\sum_{i=1}^{N} |P_\mathrm{i} - O_\mathrm{i}|}{N},$$

where P is predicted value, O is observed value, and N is number of samples.

[43] Table 2a enumerates the MBE as well as the RMSE of daily mean temperature between simulations of models at different levels and the observational data over 7 months at the D105 site. The statistics for the soil temperature and volumetric soil water content over 2 months at the D66 site are listed in Table 2b. The results in Tables 2a and 2b show that level 2.5, level 3.5, and level 4.5 models have consistently better performance in simulating temperature and soil liquid water content than the corresponding level 2, level 3, and level 4 models, regardless of the soil depths. Simulation differences between the level 2.5 (or 3.5 or 4.5) model and the level 2 (or 3 or 4) model are much larger than those between different level models (such as between level 3.5 and level 4.5), indicating that the adequate treatment of mass and thermal equations in the frozen soil model is crucially important. Model performance at the Rosemount site is very similar and therefore is not listed.

[44] There is a little difference in the simulation of soil temperature among different level models at the D105 site, which may be caused by not taking snow processes into account (Figure 2). We will improve this feature through further study. Correlation coefficients of soil temperature between simulation and observation at different depths at the D105 site are around 0.6 after removing monthly means. At the D66 site, the simulation differences between level 2 and level 3 models or between level 2.5 and level 3.5 models are small. However, the level 2 (or 2.5) and level 3 (or 3.5) models consistently show better performance than the level 4 (or 4.5) model at the top soil surface. The RMSE of temperature with the level 4.5 model is greater than that of the level 3.5 model by 0.26°C and the difference between the RMSEs of volumetric soil liquid water content can reach 0.02 m^3/m^3.

[45] To understand the cause for this improvement, volumetric soil liquid water contents at 4 cm simulated by the level 3.5 model and the level 4.5 model at the D66 site from 1 September to 1 November 1997 are compared to each other (Figure 3a). Since the level 3.5 model's simulation is very close to observations (Figures 1c and 1d), Figure 3a indicates that the level 4.5 model produces a systematic

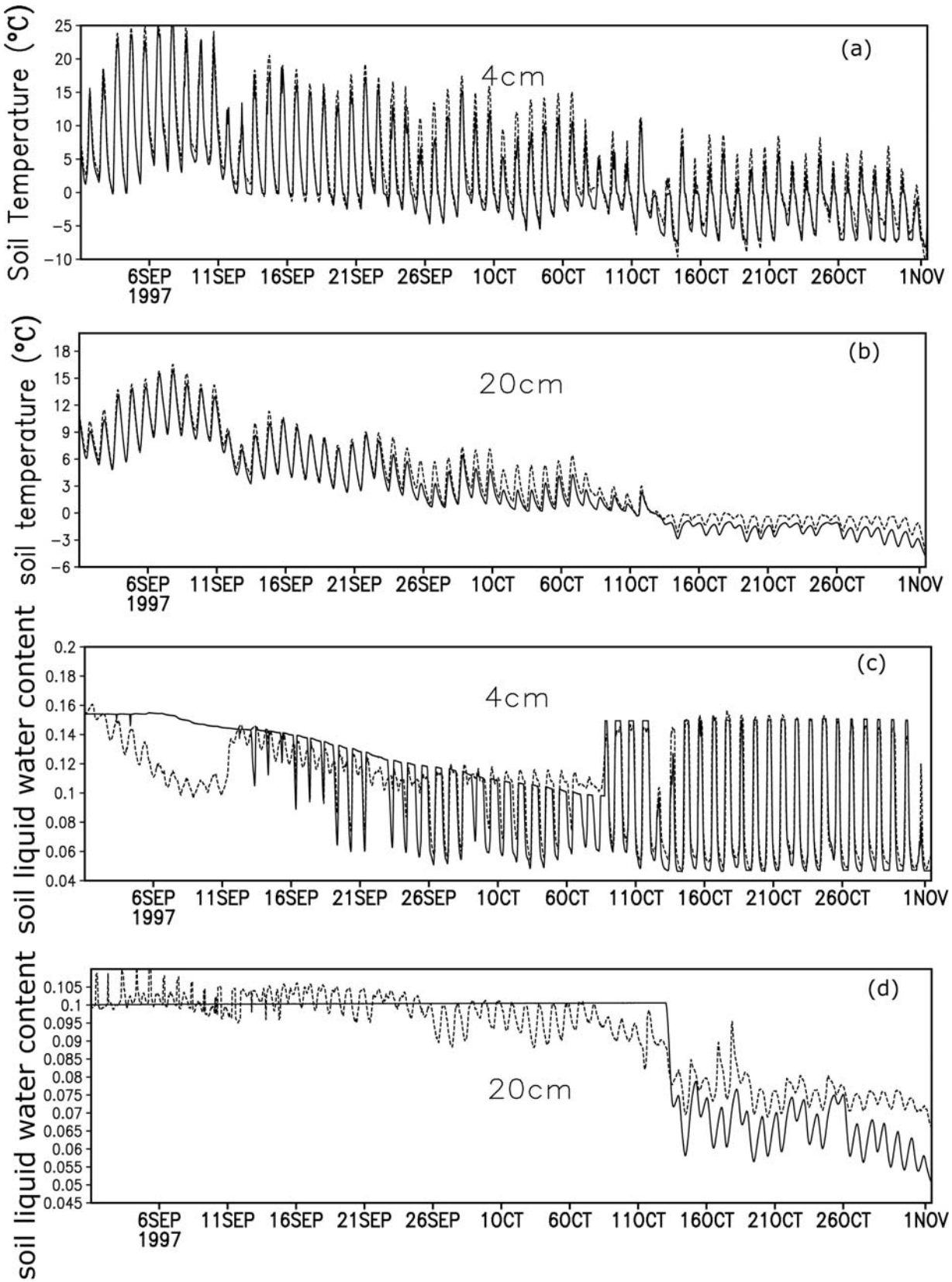

Figure 1. Comparison of observations (dashed lines) and level 3.5 model simulation (solid lines) at the D66 site. (a) Soil temperature (°C) at 4 cm, (b) soil temperature (°C) at 20 cm, (c) volumetric soil liquid water content at 4 cm, and (d) volumetric soil liquid water content at 20 cm.

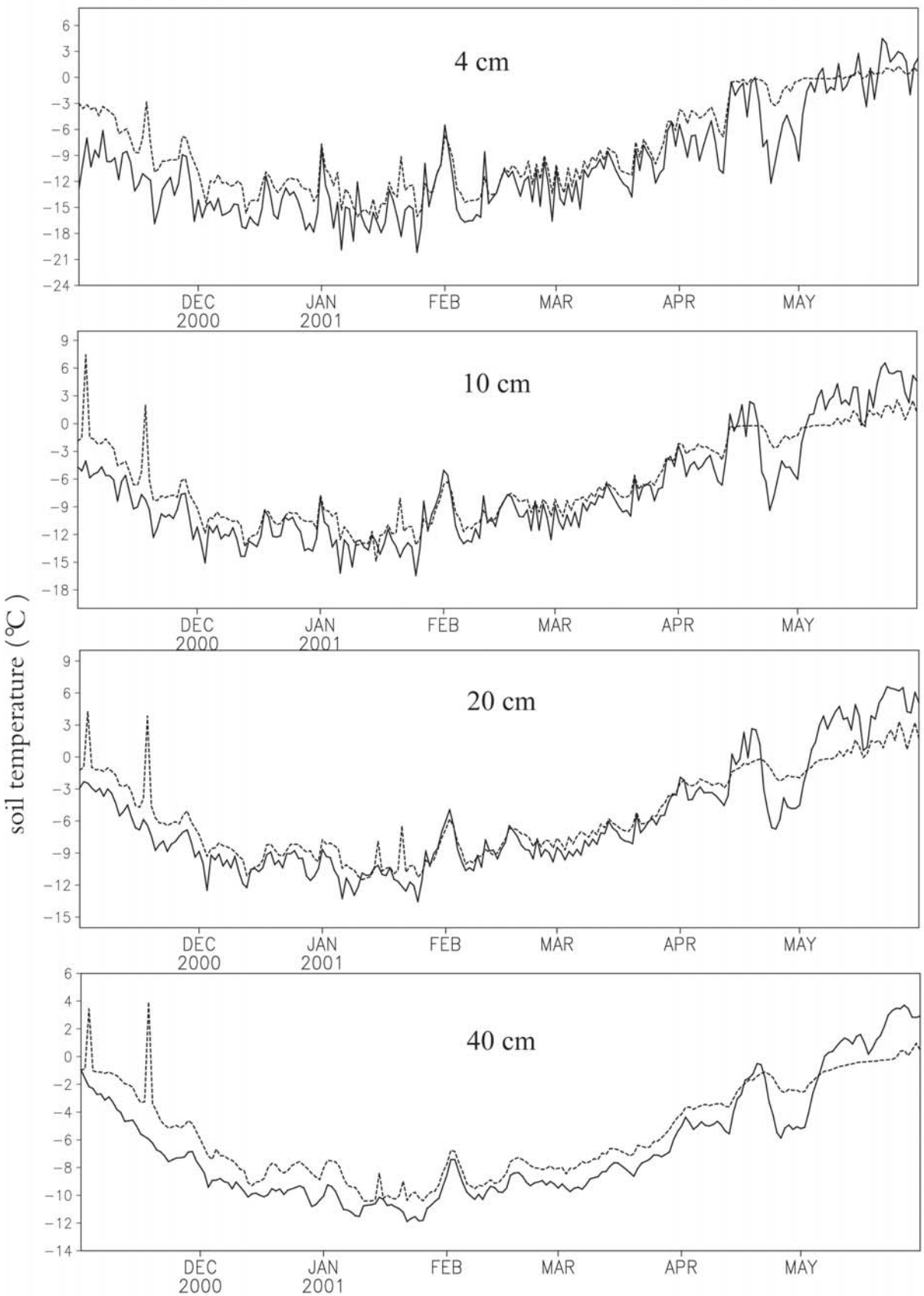

Figure 2. Soil temperature (°C) from the level 3.5 model simulation (solid lines) and observations (dashed lines) at different depths at the D105 site.

Table 2a. RMSE and MBE of Simulations by Models at Different Levels at the D105 Site

		Temperature (°C)	
Model	Tibet/D105	MBE	RMSE
Level 2	4 cm	4.030	4.813
	10 cm	4.332	4.987
	20 cm	4.082	4.686
	40 cm	3.778	4.126
Level 2.5	4 cm	2.280	2.846
	10 cm	1.529	2.115
	20 cm	1.066	1.571
	40 cm	1.260	1.586
Level 3	4 cm	4.027	4.811
	10 cm	4.331	4.985
	20 cm	4.088	4.690
	40 cm	3.801	4.147
Level 3.5	4 cm	2.321	2.809
	10 cm	1.623	2.147
	20 cm	1.216	1.648
	40 cm	1.524	1.769
Level 4	4 cm	4.026	4.810
	10 cm	4.332	4.985
	20 cm	4.090	4.693
	40 cm	3.803	4.149
Level 4.5	4 cm	2.408	2.886
	10 cm	1.653	2.173
	20 cm	1.215	1.653
	40 cm	1.471	1.705

bias. During this time period, the soil water experiences unfreezing and freezing (Figure 1). Soil begins freezing at 4 cm on 13 September (Figure 3b) and at 1 cm on 8 October (not shown). After 13 September, the difference in the volumetric soil liquid water content at 4 cm starts to appear and remains during the daytime but disappears at night. The difference in the volumetric soil ice content at 4 cm, however, appears at night but disappears during the daytime (Figure 3b). The difference between the level 3 (or 3.5) model and the level 4 (or 4.5) model is attributed to the inclusion of the contribution of vapor transport to the water balance equation in the level 3 (or 3.5) model (equation (11)) as opposed to the level 4 (or 4.5) model. We calculate every component in the vertical water flux to check the contribution of vapor transport during this process.

[46] Figure 4 shows the magnitudes and variations of different vertical flux components composing the total water flux for the periods 15–16 September and 14–15 October. Figures 4a and 4b, which represent the situation during daytime and night before the precipitation event on 8 October 1997, show that the contribution of the vapor flux is much higher than that of the liquid flux. Especially, the contribution of vapor transport (QMV) caused by the soil matric potential gradient between the 1 cm layer and the 4 cm layer dominates the total water flux at the interface of the two top soil layers. During the daytime, upward flux due to QMV at 4 cm is so large that the water content simulated by the level 3.5 model at 4 cm is lower than that simulated by the level 4.5 model (Figure 3a), in which QMV has been omitted from the water balance equation. At night, the soil liquid water begins freezing. However, the maximum liquid water content in the soil is limited by equation (8) while freezing. That is why at night the volumetric liquid water contents at 4 cm simulated by the level 4.5 and level 3.5 models are close to each other (Figure 3a). More liquid water produced by the level 4.5 model during the daytime, along with the relatively large contribution of QMV to the total water flux at night (Figure 4b), leads to more ice at night (Figure 3b). This QMV effect produces a clear decreasing trend of the total water content, and a difference in the total water content between the level 4.5 and level 3.5 simulations reaches a maximum before the precipitation event on 8 October 1997,

$$\theta_{\mathrm{l}\max} = \theta_{\mathrm{s}} \cdot \left[\frac{L_{\mathrm{i,l}} \cdot (T - T_{\mathrm{f}})}{g\psi_{\mathrm{o}} T_{\mathrm{f}}}\right]^{-1/b} \quad (T < T_{\mathrm{f}}). \tag{18}$$

[47] After precipitation, the total soil water content increases in the simulations of both models but the difference in the liquid water content between the two model simulations stays the same as before the precipitation. This is because the contribution of QMV becomes smaller owing to a dramatically reduced soil matric potential gradient at the soil surface (Figures 4c and 4d). In addition, although another component of vapor flux caused by the temperature gradient (QTV) becomes dominant in the total flux at the top soil layer, QTV (Figures 4c and 4d) is 1 order of magnitude smaller than QMV in September (Figures 4a and 4b) and cannot make a real contribution to the total water flux.

[48] At the D105 site, the forcing data (and the integration) start after freezing, and no such difference as observed at the D66 site during the melting and freezing period is found. The contribution of the gradient between the soil matric potentials should be further evaluated with long-term simulations and under snow conditions with more sites from different climate conditions. Nevertheless, this D66 case indicates that the term representing vapor transport should

Table 2b. RMSE and MBE of Simulations by Models at Different Levels at the D66 Site

		Temperature (°C)		Liquid Water Content (m^3/m^3)	
Model	Tibet/D66	MBE	RMSE	MBE	RMSE
Level 2	4 cm	1.10	1.44	0.011	0.014
	20 cm	0.75	0.89	0.004	0.006
	60 cm	0.45	0.50	0.008	0.010
	100 cm	0.26	0.30	0.004	0.004
Level 2.5	4 cm	1.04	1.35	0.013	0.016
	20 cm	0.46	0.59	0.007	0.009
	60 cm	0.25	0.29	0.008	0.011
	100 cm	0.13	0.16	0.004	0.004
Level 3	4 cm	1.10	1.43	0.011	0.014
	20 cm	0.74	0.88	0.004	0.006
	60 cm	0.44	0.49	0.008	0.010
	100 cm	0.25	0.29	0.004	0.004
Level 3.5	4 cm	1.02	1.32	0.014	0.016
	20 cm	0.44	0.56	0.008	0.009
	60 cm	0.22	0.27	0.008	0.011
	100 cm	0.12	0.14	0.004	0.004
Level 4	4 cm	1.37	1.81	0.044	0.050
	20 cm	0.65	0.79	0.005	0.006
	60 cm	0.37	0.42	0.008	0.011
	100 cm	0.19	0.23	0.004	0.004
Level 4.5	4 cm	1.20	1.58	0.032	0.036
	20 cm	0.47	0.59	0.007	0.008
	60 cm	0.23	0.27	0.008	0.011
	100 cm	0.19	0.15	0.004	0.004

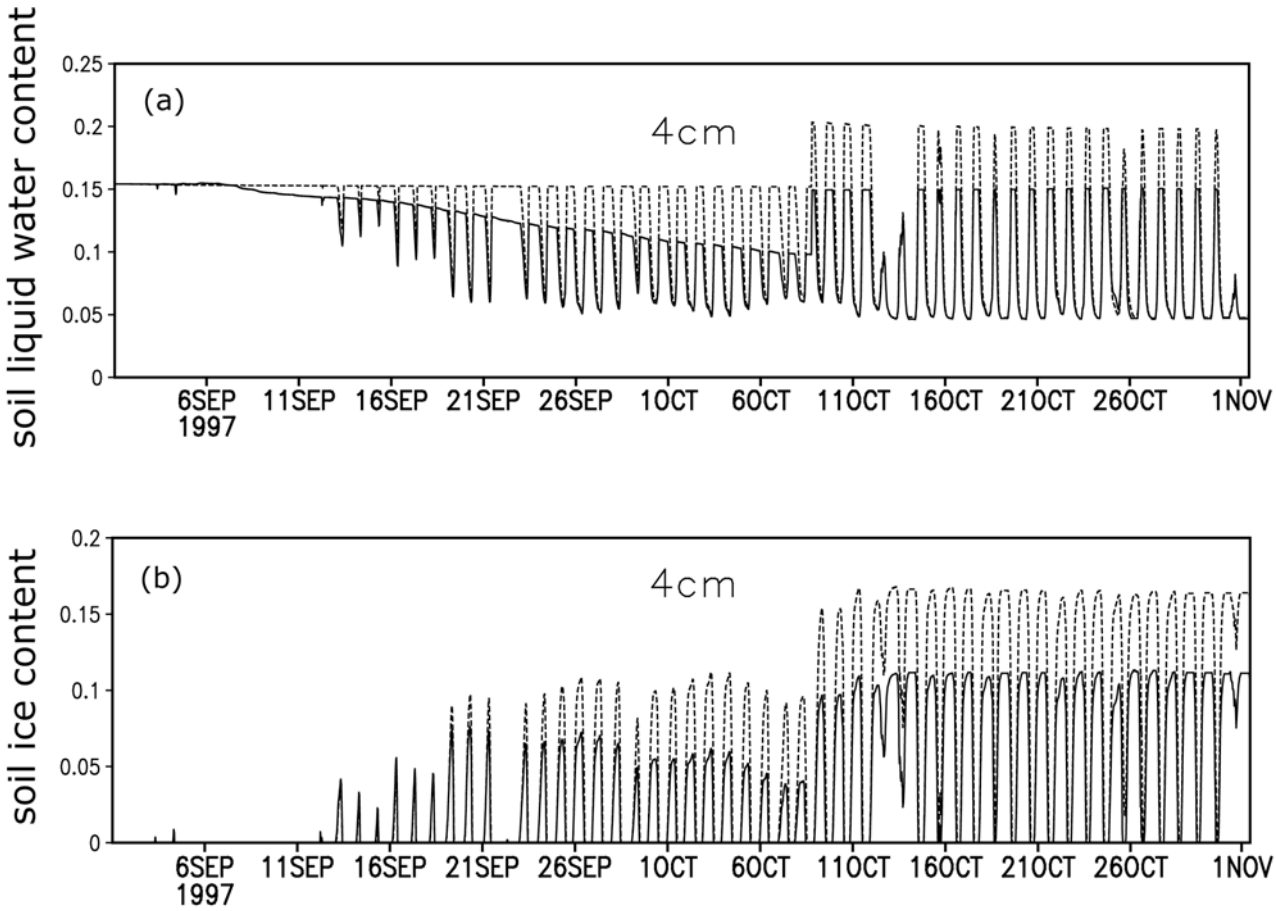

Figure 3. Comparison of simulated (a) volumetric soil liquid water content and (b) volumetric soil ice content at 4 cm between the level 3.5 model (solid line) and the level 4.5 model (dashed line) at the D66 site.

be kept in the frozen soil model for applications over broader climate conditions.

4.3. Sensitivity of Frozen Soil Process Simulations to Freezing-Melting Process Parameterizations

[49] In order to demonstrate the impact of freezing-melting process parameterizations on the simulations of the distributions of temperature and liquid water in soil and latent and sensible heat fluxes, three sensitivity studies with two very different parameterizations have been conducted: one assumes a fixed freezing point and the other is based on a thermal equilibrium assumption in frozen soil. For the fixed freezing point, two cases are examined. The first case, referred to as scheme A, assumes that the freezing point is 0°C; that is, soil liquid content is set to complete freezing at 0°C. The second case, referred to as scheme B, assumes that the freezing point is at −2°C. If a freezing-melting process parameterization has a freezing range between 0° and −2°C, the results should be between those in schemes A and B. Another case, based on a thermal equilibrium assumption, referred to as scheme C, applies method 4 in section 3. Please note that method 1 presented in section 3 is equivalent to scheme A. The results from method 2 in section 3 should be between the results obtained using schemes A and B. On the basis of the performances of models at different levels discussed in section 4.2, the level 3.5 model was chosen to conduct the sensitivity study.

[50] The numerical sensitivity study for these three schemes uses the D66 site and Rosemount site data sets described above. Since the conclusions with the two data sets are similar, only the numerical results from the Rosemount Station data are discussed in this paper. The effects of different freezing-melting schemes on the results are more evident during the period of soil freezing and melting, so we only select the time period from 1 November to 5 November 1996 to clearly demonstrate the impact of freezing-melting parameterization on frozen soil process simulation.

[51] Figures 5 and 6 display the comparisons of simulated temperature, volumetric liquid water content, sensible heat fluxes, and latent heat fluxes at the soil surface layer between schemes A and C and between B and C, respectively. For scheme A, when the soil surface temperature decreases to 0°C, the soil begins to freeze and the temperature remains at 0°C until all liquid water becomes ice (Figure 5a). Afterward, there is no liquid water content as long as the soil temperature is below 0°C (Figure 5b). Many results from laboratory experiments or field observations [e.g., *Beskow*, 1935] have indicated that this is not in accord

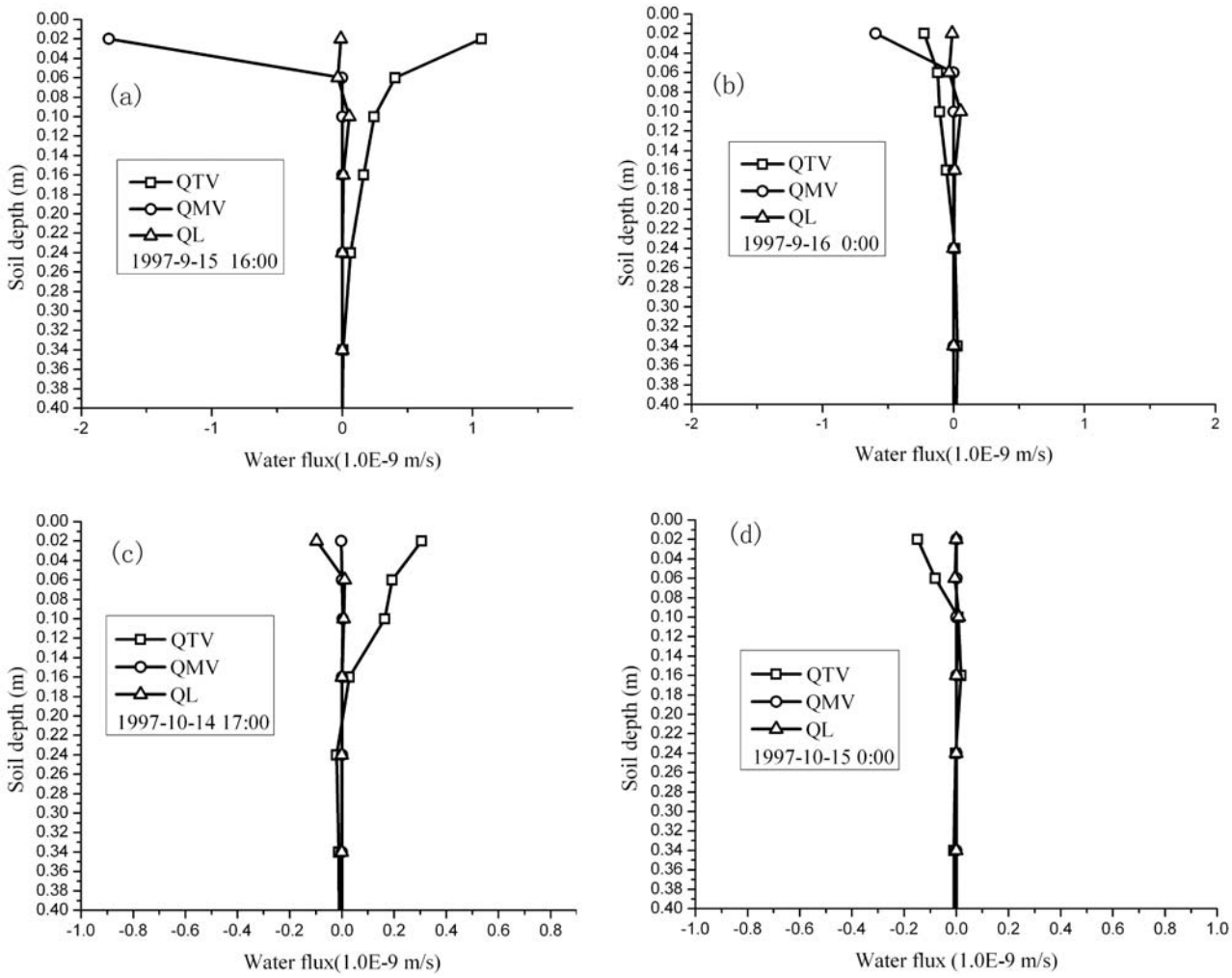

Figure 4. Simulated vertical water fluxes (10^{-9} m/s) at the D66 site by the level 3.5 model (a) at 1600 local time (LT), 15 September 1997, (b) at 0000 LT, 16 September 1997, (c) at 1700 LT, 14 October 1997, and (d) at 0000 LT, 15 October 1997. QTV and QMV: the fluxes due to vapor transport caused by the temperature gradient and soil matric potential, respectively; QL: liquid water flux.

with what is actually happening in frozen soil in most cases. For scheme C, soil liquid water does not start to freeze at 0°C and the soil temperature gradually reduces and passes through 0°C (Figure 5a). Compared to scheme A, scheme C has a much shorter time period with temperature at 0°C. Furthermore, with scheme C, liquid water begins to freeze at some temperature below 0°C and the freezing process proceeds gradually. Liquid water content never vanishes, which leads to more liquid water content and less ice content calculated from scheme C in soil than from scheme A (Figure 5b). All these details are consistent with observations. Because of the difference in temperature and liquid water content between the two schemes, the sensible and latent heat fluxes between the two schemes are also quite different (Figures 5c and 5d). Large differences occur during the daytime. The results from scheme B (Figure 6) are similar to the result from scheme A (Figure 5), except that the frozen temperature is at −2°C. In addition, we calculated the differences of simulated mean and maximum heat fluxes as well as the root-mean-squared difference between schemes A and C and between schemes B and C. The maximal differences in sensible heat fluxes are quite substantial and can reach 189 W/m^2 between schemes A and C and 123 W/m^2 between schemes B and C. As for the latent heat flux, the maximal differences between schemes A and C and between schemes B and C are 69 and 49 W/m^2, respectively. The substantial difference between sensible and latent fluxes simulated by schemes A, B, and C has important implications for frozen soil or cold season climate interaction studies.

[52] The results in this section indicate that results from methods 1 and 2 are inconsistent with the observational facts, which limits the application of these methods in spite of their simplicity and convenience in computation in the frozen soil model. Method 4 is more applicable under a wide range of conditions. Its superior performance is consistent with soil physical principles.

[53] From the viewpoint of soil physics, all phases in the frozen soil system are under the assumption of thermal equilibrium [*Zhao et al.*, 1997]. The freezing-point depres-

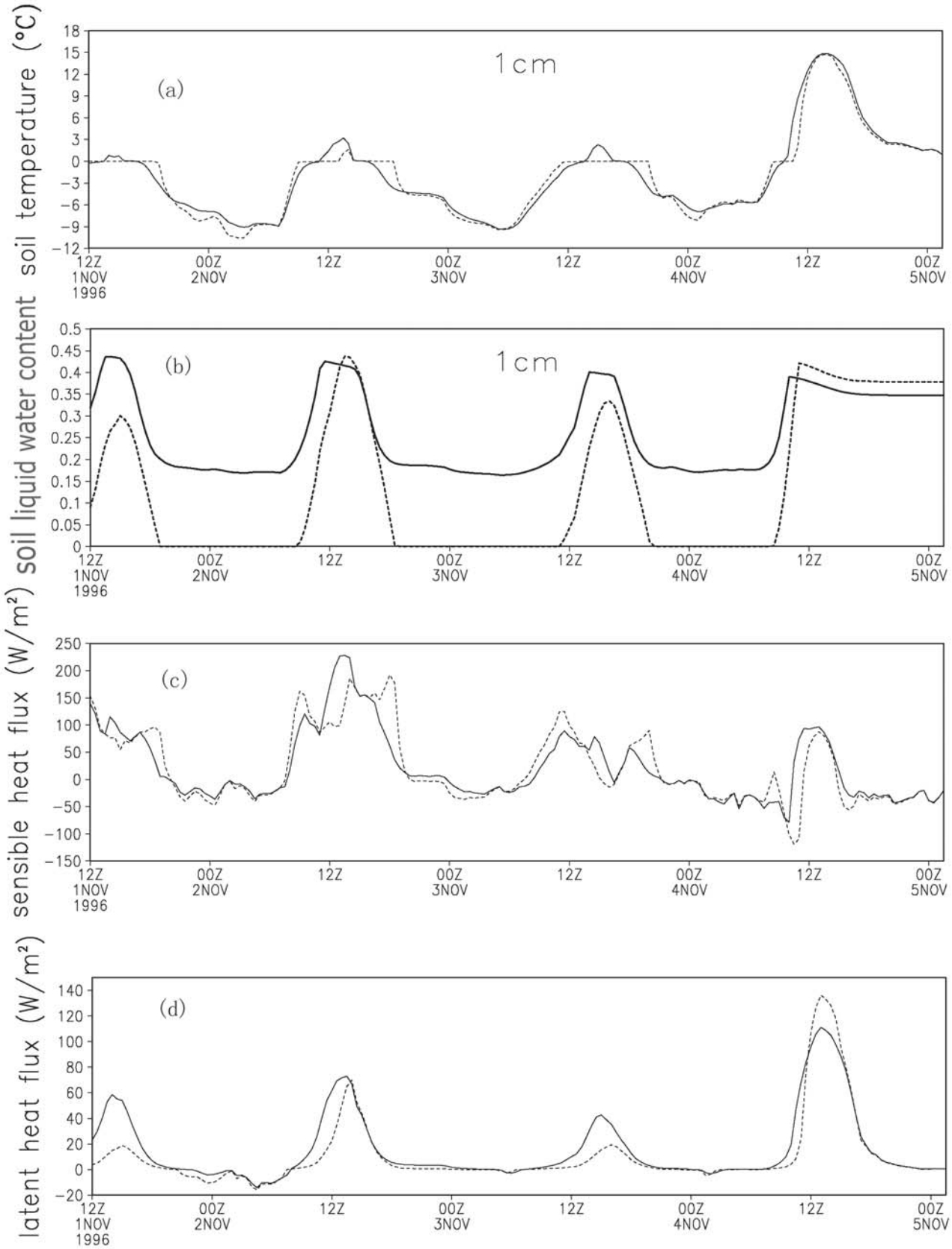

Figure 5. Comparison of (a) soil surface temperature (°C), (b) volumetric liquid water content, (c) sensible heat flux (w/m^2), and (d) latent heat flux (w/m^2) at the soil surface simulated by scheme A (dashed lines) and scheme C (solid lines) at the Rosemount Station.

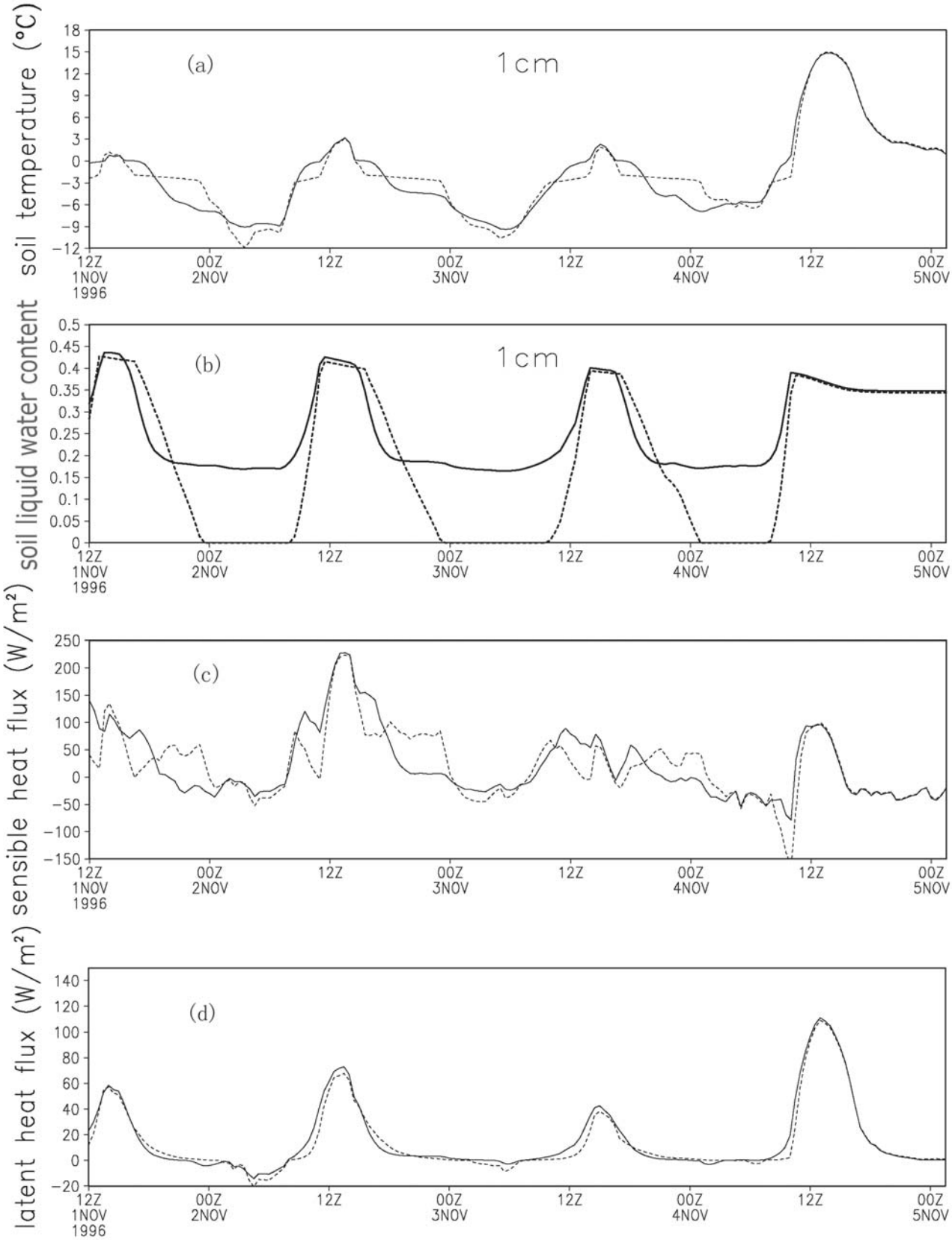

Figure 6. Comparison of (a) soil surface temperature (°C), (b) volumetric liquid water content, (c) sensible heat flux (w/m^2), and (d) latent heat flux (w/m^2) at the soil surface simulated by scheme B (dashed lines) and scheme C (solid lines) at the Rosemount Station.

sion relation such as depicted in equation (8) is derived from that assumption and has been widely used by the soil physics community. It is a basic relation and needs to be followed if the equilibrium assumption is accepted. In fact, so far, most research work in the soil physics field is based on the thermodynamic equilibrium assumption because the knowledge required to deal with the nonequilibrium thermodynamic problem in frozen soil is very limited. Therefore, if we consider the empirical freezing-melting process relationship, such as by using method (3), as an independent one, it means that we must rederive the soil matric potential relation (equation 6) from the freezing point depression relationship (equation 8) and the empirical freezing-melting process relationship. However, the relationship of hydraulic characteristics presented in equation (6) is an intrinsic constitutive one for unsaturated unfrozen and frozen soil physics and has been used in soil physics for a long time. Even though equation (6) cannot be derived from a theoretical base, this semiempirical relation was built on a physical base and created with a large amount of available data for different soil textures and has been widely acknowledged by the soil physics community as an acceptable and useful relation. Therefore, we believe that method 4 is more justified than the other three schemes.

[54] We did not test method 3 because a quite different numerical scheme would have to be designed. Most analyses of method 3 seem to perform very well with the validation data. However, they are empirical relations based on only limited data available from laboratory or field measurements. Caution must be taken when extending their application to a much larger scale or an area without validation.

5. Conclusions and Discussion

[55] In this paper, models at different levels associated with different complexities in the governing equations are presented. We derive equations at different levels hierarchically based on scale analysis and discuss the rationality for the simplification of the models of different levels. In this paper, level 1, level 2, level 3, and level 4 models represent decreasing complexity in the governing equations. The complexity and one unproven assumption in the level 1 model limit its applicability in the study of frozen soil, even though a detailed description of all processes is included. Preliminary evaluations of the performance of the different level models are conducted with three observational data sets. In order to deal with the phase change between liquid and ice more efficiently, we propose a variable transformation approach introducing enthalpy and total water mass in the prognostic equations as substitutes for temperature and liquid water content in level 2, level 3, and level 4 models. We refer to these new models as level 2.5, level 3.5, and level 4.5, respectively. Comparisons of simulated results with observational data show that simulation results from the level 2.5, level 3.5, and level 4.5 models are consistently better than those from the level 2, level 3, and level 4 models, respectively.

[56] In our limited testing, simulated soil temperature by different level models shows good agreement with observational data at the D105 site, with a correlation coefficient of about 0.6. However, there are some disagreements from April to May 2001 with thawing snow that need to be further investigated with a coupled snow model. At the D66 site, level 2 (or 2.5), level 3 (or 3.5), and level 4 (or 4.5) models produce similar accuracy except at the top soil layer. We attribute this difference to the inclusion of vapor transport due to the matric potential in level 2 (or 2.5) and level 3 (or 3.5) models, which forces these models to have a different frozen or melting cycle compared to the level 4 (or 4.5) model.

[57] Furthermore, the rationale for using different freezing-melting process schemes is discussed. Observations and simulation results indicate that the earlier closure methods (methods 1 and 2) are generally unrealistic. Method 3 can produce good performance when an appropriate empirical relationship between soil temperature and unfrozen soil water or ice content is chosen. But its validity relies on the observational data that are used to derive the empirical relation. This paper has shown that the model derived from the freezing-point depression equation and soil matric potential equation is supported by both thermodynamic equilibrium theory and the simulation results and is suitable for climate studies. Recently, there has been increasing awareness of the important role of soil macropores in controlling hydraulic and thermal processes in frozen soil. The soil in the real world may contain particles of different sizes and thus may form micropores, mesopores, and/or macropores. Fine soil particles (or micropores) exert the most capillary forces to adsorb liquid water in frozen soil, while structured or aggregated soil (with macropores) does not. Method 4 may result in more liquid water in frozen soil and require iterations to solve for the liquid water content. In some sites in Alaska, there was not much liquid water in frozen soil because of large soil particles. Since this study only tests models and schemes with very limited data, further investigation with more available data, including snow cover conditions, is necessary.

Appendix A

[58] Equation (3) is examined to simplify the level 1 model. In the equation, the order of magnitude of the first term on the left-hand side can be estimated as follows:

$$O\left(\frac{\partial \theta_v \rho_v}{\partial t}\right) = O\left(\overline{\theta}_v \cdot \frac{\partial \rho_v}{\partial T} \cdot \frac{\partial T}{\partial t}\right) = \overline{\theta}_v O\left(\frac{\partial \rho_v}{\partial T}\right) \cdot O\left(\frac{\partial T}{\partial t}\right) \quad \text{(A1)}$$

and the order of magnitude of the term on the right-hand side is

$$\begin{aligned} O\left[\frac{\partial}{\partial Z}\left(D_{\text{eff}} \frac{\partial \rho_v}{\partial Z}\right)\right] &= O(D_{\text{eff}}) \cdot O\left[\frac{\partial}{\partial Z}\left(\frac{\partial \rho_v}{\partial Z}\right)\right] \\ &= O(D_{\text{eff}}) \cdot O\left[\frac{\partial}{\partial Z}\left(\frac{\partial \rho_v}{\partial T}\frac{\partial T}{\partial Z}\right)\right] \\ &= \overline{\theta}_v \cdot \frac{D_V}{\tau}\left\{O\left(\frac{\partial \rho_v}{\partial T}\right) \cdot O\left[\frac{\partial}{\partial Z}\left(\frac{\partial T}{\partial Z}\right)\right] \right. \\ &\quad \left. + O\left[\frac{\partial}{\partial Z}\left(\frac{\partial \rho_v}{\partial T}\right)\right] \cdot O\left(\frac{\partial T}{\partial Z}\right)\right\}, \end{aligned} \quad \text{(A2)}$$

where O denotes the order of terms and $D_{\text{eff}} = \frac{\theta_v}{\tau} D_v$ represents the vapor effective diffusivity constant.

Table B1. Values of Items in Governing Equations with Different Volumetric Liquid Water Content, Ice Content, and Soil Temperature for Clay[a]

	θ_l (m^3/m^3)	θ_i (m^3/m^3)	K_l (m/s)	D_{TV}/ρ_l (m^2/K/s)	$D_{\psi V}/\rho_l$ (m/s)	K_{eff} (J/K/m/s)	$L_{lv}D_{\psi V}$ (J/m^2/s)	$L_{lv}D_{TV}$ (J/m/K/s)	$\rho_l c_l K_l T$ (J/m^2/s)	$\frac{\partial\psi}{\partial Z}$
$T = -2.069°C$	0.15	0	1.20E−19	3.40E−14	3.10E−17	9.60E−01	7.80E−08	8.40E−05	−1.10E−12	1.80E+07
	0.25	0	7.60E−14	9.10E−13	1.00E−15	1.30E+00	2.50E−06	2.30E−03	−6.60E−07	3.00E+04
	0.3	0.1	2.80E−13	3.30E−13	0.00E+00	1.80E+00	0.00E+00	8.30E−04	−2.40E−06	9.90E+03
	0.309	0.14	1.50E−13	9.50E−14	0.00E+00	2.00E+00	0.00E+00	2.40E−04	−1.30E−06	9.60E+03
$T = -10.281°C$	0.15	0	1.20E−19	1.70E−14	1.50E−17	9.60E−01	3.70E−08	4.10E−05	−5.30E−12	1.80E+07
	0.25	0.05	1.40E−14	4.20E−13	0.00E+00	1.30E+00	0.00E+00	1.10E−03	−5.80E−07	5.90E+04
	0.261	0.1	7.50E−15	2.70E−13	0.00E+00	1.60E+00	0.00E+00	6.70E−04	−3.20E−07	5.70E+04
	0.27	0.15	3.30E−15	1.20E−13	0.00E+00	2.00E+00	0.00E+00	3.00E−04	−1.40E−07	5.50E+04
$T = -20.72°C$	0.15	0	1.20E−19	6.30E−15	5.30E−18	9.60E−01	1.30E−08	1.60E−05	−1.10E−11	1.80E+07
	0.238	0.062	2.50E−15	1.70E−13	0.00E+00	1.30E+00	0.00E+00	4.20E−04	−2.10E−07	1.30E+05
	0.246	0.1	1.50E−15	1.20E−13	0.00E+00	1.60E+00	0.00E+00	3.10E−04	−1.30E−07	1.20E+05
	0.254	0.15	6.80E−16	6.40E−14	0.00E+00	1.90E+00	0.00E+00	1.60E−04	−5.90E−08	1.20E+05
$T = -25.388°C$	0.15	0	1.20E−19	3.90E−15	3.30E−18	9.60E−01	8.20E−09	9.90E−06	−1.30E−11	1.80E+07
	0.233	0.06	1.60E−15	1.10E−13	0.00E+00	1.30E+00	0.00E+00	2.90E−04	−1.70E−07	1.60E+05
	0.25	0.15	4.30E−16	4.50E−14	0.00E+00	1.90E+00	0.00E+00	1.10E−04	−4.50E−08	1.50E+05

[a]Units of measure: volumetric liquid water content, m^3/m^3; ice content, m^3/m^3; and soil temperature, °C.

[59] Because the value of the second term on the right-hand side in (A2) is very small due to the small vertical variation of $\frac{\partial\rho_v}{\partial T}$, the ratio R of (A1) to (A2) is

$$R = \bar{\theta}_v O\left[\frac{\partial\rho_v}{\partial T}\right] O\left[\frac{\partial T}{\partial t}\right] \Big/ \bar{\theta}_v \frac{D_V}{\tau} O\left[\frac{\partial\rho_v}{\partial T}\right] \cdot O\left[\frac{\partial^2 T}{\partial Z^2}\right] = O\left[\frac{\partial T}{\partial t}\right] \Big/ \frac{D_V}{\tau} \cdot O\left[\frac{\partial^2 T}{\partial Z^2}\right]. \quad \text{(A3)}$$

For the diurnal change of temperature around the soil surface, the characteristic length scale (L_d) estimated on the basis of molecular conduction theory is about 0.1 m [*Robinson and Henderson-Sellers*, 1999]. The terms in (A3) are

$$O\left[\frac{\partial T}{\partial t}\right] \sim O\left[\frac{\Delta T}{t_{\text{diurnal}}} = \frac{\Delta T}{86,400\,\text{s}}\right] \sim O\left[\frac{\Delta T \cdot 10^{-5}}{\text{s}}\right]$$

$$\frac{D_V}{\tau} \cdot O\left[\frac{\partial^2 T}{\partial Z^2}\right] \sim O\left[\frac{\Delta T}{L_d^2}\right] \cdot \frac{D_V}{\tau} \sim O\left[\frac{\Delta T}{0.1m \cdot 0.1m} \cdot 4 \times 10^{-5}\ \text{m/s}\right] \sim O\left[\Delta T \cdot 4 \times 10^{-3}/\text{s}\right],$$

where ($D_V = 2 \times 10^{-5}$ m^2/s) and $\tau = O(0.5)$. Thus, R has an order of magnitude of 10^{-2}.

[60] Similarly, the annual temperature wave has damping depth L_a = 4 m [*Robinson and Henderson-Sellers*, 1999] and t_{annual} = 86,400 × 365 s, and then

$$O\left[\frac{\partial T}{\partial t}\right] \sim O\left[\frac{\Delta T}{86,400 \times 365\,\text{s}}\right] \sim O\left[\frac{\Delta T \cdot 10^{-8}}{\text{s}}\right],$$

$$\frac{D_V}{\tau} \cdot O\left[\frac{\partial^2 T}{\partial Z^2}\right] \sim O\left[\frac{\Delta T}{4m \cdot 4m}\right] \cdot \frac{D_V}{\tau} \sim O\left[\frac{\Delta T}{4m \cdot 4m} \cdot 4 \times 10^{-5}\ \text{m}^2/\text{s}\right] \sim O\left[\Delta T \cdot 10^{-6}/\text{s}\right].$$

It is clear that R also equals 10^{-2} when considering the annual change of temperature in soil. Therefore, the term (A2) can be eliminated in equation (3).

Appendix B

[61] Scale analysis of the order of magnitude of various flux terms in the energy and mass balance equations in the level 2 model (equations (11) and (12)) is carried out and discussed in this section.

[62] In the mass and heat balance equations of the level 2 model, there are six items related to the water and heat fluxes. They are

$$Q_L = -K_l \frac{\partial\psi}{\partial Z} + K_l, \quad Q_{MV} = -D_{\psi V}\frac{\partial\psi}{\partial Z}, \quad Q_{TV} = -D_{TV}\frac{\partial T}{\partial Z},$$

$$QH_{\text{conduct}} = -K_{\text{eff}}\frac{\partial T}{\partial Z}, \quad QH_{\text{convect}} = \rho_l c_l T K_l\left(1 - \frac{\partial\psi}{\partial Z}\right),$$

$$\text{and} \quad QH_{\text{vapor}} = -\left(L_{l,v}D_{\psi V}\frac{\partial\psi}{\partial Z} + L_{l,v}D_{TV}\frac{\partial T}{\partial Z}\right),$$

where Q_L, Q_{MV}, and Q_{TV} are the liquid flux and vapor diffusion fluxes in the mass balance equation (equation (11)) and QH_{conduct}, QH_{convect}, and QH_{vapor} are the heat fluxes due to thermal conductivity (the third term on the right-hand side in equation (12)), the heat flux due to liquid movement (the first term on the right-hand side in equation (12)), and the heat flux from energy released or absorbed by the phase change of vapor (the second term on the right-hand side in equation (2.4)), respectively. The importance of these terms in the equations is determined by the relative magnitudes of K_l, D_{TV}/ρ_l, $D_{\psi V}/\rho_l$, K_{eff}, $L_{l,V}D_{\psi V}$, $L_{l,v}D_{TV}$, and $\rho_l c_l K_l T$ together with the ratio of $\frac{\partial T}{\partial Z}$ to $\frac{\partial\psi}{\partial Z}$. The values of these terms for six soil textures (sand, sandy loam, loam, silt loam, sandy clay, and clay) with different soil liquid water contents and different temperatures have been calculated and analyzed. Tables B1 and B2 show results for clay and sand soil as representative examples.

[63] In Tables B1 and B2, the order of magnitude of $\frac{\partial\psi}{\partial Z}$ and $\frac{\partial T}{\partial Z}$ are estimated as follows. The magnitude order of $\frac{\partial T}{\partial Z}$ in diurnal variation is about O (10°C/0.1 m = 100°C/m). The magnitude order of $\frac{\partial\psi}{\partial Z}$ varies with soil textures and soil liquid water content and can be estimated by the order of magnitude of $\frac{\partial\psi}{\partial\theta_l}$ and $\frac{\partial\theta_l}{\partial Z}$ ($\frac{\partial\psi}{\partial Z} = \frac{\partial\psi}{\partial\theta_l} \cdot \frac{\partial\theta_l}{\partial Z}$). $O\left(\frac{\partial\psi}{\partial\theta_l}\right)$ can be estimated from the relationship of $\psi - \theta_l$ expressed in equation (6) and $O\left(\frac{\partial\theta_l}{\partial Z}\right) = O(0.1/0.1\ \text{m} = 1/1\ \text{m})$ is considered as a reasonable and realistic estimation [*Sun et al.*, 2003] So there is the following relationship:

$$O\left(\frac{\partial\psi}{\partial Z}\right) = O\left(\frac{\partial\psi}{\partial\theta_l} \cdot \frac{\partial\theta_l}{\partial Z}\right) = O\left(\frac{\partial\psi}{\partial\theta_l}\right) O(1/\text{m}).$$

Table B2. Values of Items in Governing Equations With Different Volumetric Liquid Water Content, Ice Content, and Soil Temperature for Sand[a]

	θ_l (m^3/m^3)	θ_i (m^3/m^3)	K_l (m/s)	D_{TV}/ρ_l (m^2/K/s)	$D_{\psi V}/\rho_l$ (m/s)	K_{eff} (J/K/m/s)	$L_{lv}D_{\psi V}$ ($J/m^2/s$)	$L_{lv}D_{TV}$ (J/m/K/s)	$\rho_l c_l K_l T$ ($J/m^2/s$)	$\frac{\partial\psi}{\partial Z}$
$T = -2.044°C$	0.015	0	2.60E−18	1.40E−12	1.50E−15	5.80E−01	3.90E−06	3.50E−03	−2.20E−11	7.70E+04
	0.025	0.075	1.50E−17	1.20E−12	0.00E+00	1.70E+00	0.00E+00	2.90E−03	−1.30E−10	2.80E+04
	0.039	0.25	1.80E−18	2.40E−13	0.00E+00	4.40E+00	0.00E+00	6.10E−04	−1.50E−11	1.80E+04
$T = -9.98°C$	0.009	0	3.20E−20	7.30E−13	7.80E−16	5.80E−01	1.90E−06	1.80E−03	−1.30E−12	5.30E+05
	0.011	0.01	9.90E−20	8.20E−13	0.00E+00	5.50E−01	0.00E+00	2.10E−03	−4.20E−12	3.20E+05
	0.02	0.2	3.10E−20	3.10E−13	0.00E+00	3.50E+00	0.00E+00	7.70E−04	−1.30E−12	1.70E+05
$T = -20.423°C$	0.007	0	3.70E−21	2.80E−13	2.90E−16	5.80E−01	7.10E−07	7.10E−04	−3.20E−13	1.40E+06
	0.01	0.05	1.40E−20	2.90E−13	0.00E+00	1.10E+00	0.00E+00	7.20E−04	−1.20E−12	7.10E+05
	0.017	0.25	1.50E−21	7.40E−14	0.00E+00	4.30E+00	0.00E+00	1.90E−04	−1.30E−13	4.10E+05
$T = -27.542°C$	0.007	0	3.70E−21	1.60E−13	1.50E−16	5.80E−01	3.80E−07	3.90E−04	−4.30E−13	1.40E+06
	0.009	0.05	5.40E−21	1.50E−13	0.00E+00	1.10E+00	0.00E+00	3.70E−04	−6.30E−13	1.10E+06
	0.015	0.235	7.70E−22	4.80E−14	0.00E+00	4.00E+00	0.00E+00	1.20E−04	−8.90E−14	6.40E+05

[a]Units of measure: volumetric liquid water content, m^3/m^3; ice content, m^3/m^3; and soil temperature, °C.

[64] The typical values of $\frac{\partial\psi}{\partial\theta_l}$ and $\frac{\partial\psi}{\partial Z}$ with different soil liquid water contents for clay and sand are shown in Tables B1 and B2, respectively.

[65] It can be found that in the energy balance equation, the values of heat flux due to thermal conductivity are always two orders of magnitude larger than those of the latent heat flux due to the vapor phase change. Also, the heat conducted by the temperature gradient for the six soils are two orders of magnitude larger than the values of heat due to by the liquid water movement, especially when the soil is dry or deeply frozen. For the mass balance equation, the order of magnitude of water flux caused by vapor diffusion due to a temperature gradient could be comparable to that of liquid water flux depending on the soil wetness, ice content, and soil texture. And the water flux caused by vapor diffusion due to the matric potential gradient can be neglected when soil freezes because the value of $D_{\psi V}$ is zero due to the fact that the vapor density of ice in frozen soil is only a function of temperature. However, when soil thaws, the term should be considered in the model.

Notation

θ_l volumetric liquid water content (m^3/m^3).
θ_i volumetric ice content (m^3/m^3).
θ_v volumetric vapor content (m^3/m^3).
θ_s volumetric soil liquid water content at saturation (m^3/m^3).
T soil temperature (K).
Z soil depth (m).
t time (s).
ρ_l intrinsic densities of liquid (kg/m^3).
ρ_i intrinsic densities of ice (kg/m^3).
ρ_v intrinsic densities of vapor (kg/m^3).
$\dot{M}_{i,l}$ phase change rate from ice to liquid (m/s^1).
$\dot{M}_{i,v}$ phase change rate from ice to vapor (m/s^1).
$\dot{M}_{l,v}$ phase change rate from liquid to vapor (m/s^1).
C_v volumetric heat capacity ($J/m^3/K^1$).
K_l hydraulic conductivity (m/s^1).
K_{eff} effective thermal conductivity ($W/m^1/K^1$).
D_{eff} effective diffusivity of vapor.
D_{TV} vapor diffusivity due to a thermal gradient ($kg/m^2/s^1$).
$D_{\psi V}$ vapor diffusivity due to a matric potential gradient ($kg/m^1/K^1/s^1$).
u_l liquid water flow rate (m/s^1).
ψ soil matric potential (m).
$L_{i,v}$ latent heat of sublimation (J/kg^1).
$L_{l,v}$ latent heat of evaporation (J/kg^1).
$L_{i,l}$ latent heat of fusion (J/kg^1).
ψ_0 saturated soil matric potential (m).
b Clapp-Hornberger constant.
e_v local equilibrium vapor pressure (Pa).
R_v gas constant ($J/kg^1/K^1$).
g acceleration of gravity (m/s^2).
C_k coefficient of the impedance factor.
T_f freezing point of free water (273.15 K).
q_v water vapor flux ($kg/m^2/s^1$).

[66] **Acknowledgments.** This work has been supported by projects from (1) the National Natural Science Foundation of China grant 40905039, (2) the National Basic Research Program of China grant 2009CB421405, (3) The Innovation Project of the Chinese Academy of Sciences (grant KZCX2-YW-220) and the National Natural Science Foundation of China (grant 40730952), and (4) the U.S. NOAA grant NA07OAR4310226 and NSF grant NSF-ATM-0353606. Meanwhile, the authors wish to thank Degang Zhou from the Institute of Tibetan Plateau Research, Chinese Academy of Sciences, for providing the Tibet D105 data; Meixue Yang from the Cold and Arid Regions Environmental and Engineering Research Institute, Chinese Academy of Sciences, for providing the data from the Tibet D66 Station; and John M. Baker from the University of Minnesota for providing the data from Rosemount Experiment Station.

References

Baker, J. M., and R. R. Allmaras (1990), System for automating and multiplexing soil moisture measurement by time domain reflectometry, *Soil Sci. Soc. Am. J.*, *54*, 1–6.

Beskow, G. (1935), Soil freezing and frost heaving with special application to roads and railroads, *Swed. Geol. Surv. Yearb.*, *26*, 375–380.

Cary, J. W., and H. F. Mayland (1972), Salt and water movement in unsaturated frozen soil, *Soil Sci. Soc. Am. J.*, *36*, 549–555.

Celia, M. A., E. T. Bououtas, and R. L. Zarba (1990), A general mass-conservative numerical solution for the unsaturated flow equation, *Water Resour. Res.*, *26*, 1483–1496.

Cherkauer, K. A., and D. P. Lettenmaier (1999), Hydrologic effects of frozen soils in the upper Mississippi River basin, *J. Geophys. Res.*, *104*(D16), 19,599–19,610, doi:10.1029/1999JD900337.

Cox, P. M., R. A. Betts, C. D. Jones, S. A. Spall, and I. J. Totterdell (2000), Acceleration of global warming due to carbon-cycle feedbacks in a coupled climate model, *Nature*, *408*, 184–187.

Dai, Y., et al. (2003), The Common Land Model (CLM), *Bull. Am. Meteorol. Soc.*, *84*, 1013–1023.

Decker, M., and X. Zeng (2006), An empirical formulation of soil ice fraction based on in situ observations, *Geophys. Res. Lett.*, *33*, L05402, doi:10.1029/2005GL024914.

Dickinson, R. E., A. Henderson-Sellers, and P. J. Kennedy (1993), Biosphere-atmosphere transfer scheme (BATS) version le as coupled to the

NCAR community climate model, *NCAR/TN387 + STR*, Natl. Cent. for Atmos. Res., Boulder, Colo.

Elberling, B., and K. K. Brandt (2003), Uncoupling of microbial CO_2 production and release in frozen soil and its implications for field studies in Arctic C cycling, *Soil Biol. Biochem.*, *35*, 263–272.

Engelmark, H., and U. Svensson (1993), Numerical model of phase change in freezing and thawing unsaturated soil, *Nord. Hydrol.*, *24*, 95–110.

Esch, D. C., and T. E. Osterkamp (1990), Cold regions engineering: Climatic concern for Alaska, *J. Cold Reg. Eng.*, *4*, 6–14.

Ferrians, O. J., R. Kachadoorian, and G. W. Greene (1969), Permafrost and related engineering problems in Alaska, *U.S. Geol. Surv. Prof. Pap.*, *678*, 1–37.

Flerchinger, G. N., and K. E. Saxton (1989), Simultaneous heat and water model of a freezing snow-residue-soil system. Part I. Theory and development, *Trans. Am. Soc. Agric. Eng.*, *32*, 565–571.

Friedlingstein, P., L. Bopp, P. Ciais, J.-L. Dufresne, L. Fairhead, H. Le-Treut, P. Monfray, and J. Orr (2001), Positive feedback between future climate change and the carbon cycle, *Geophys. Res. Lett.*, *28*, 1543–1546.

Fuchs, M., G. S. Campbell, and R. I. Papendick (1978), An analysis of sensible and latent heat flow in a partially frozen unsaturated soil, *Soil Sci. Soc. Am. J.*, *42*, 379–385.

Guymon, G. L., and J. N. Luthin (1974), A coupled heat and moisture transport model for arctic soils, *Water Resour. Res.*, *10*, 995–1001.

Halliwell, D. H., and W. R. Rouse (1989), A comparison of sensible and latent heat flux calculations using the Bowen ratio and aerodynamic methods, *J. Atmos. Oceanic Technol.*, *6*, 563–574.

Hansson, K., J. Simunek, M. Mizoguchi, L. C. Lundin, and M. T. van Genuchten (2004), Water flow and heat transport in frozen soil: Numerical solution and freeze/thaw applications, *Vadose Zone J.*, *3*, 693–704.

Harlan, R. L. (1973), Analysis of coupled heat-fluid transport in partially frozen soil, *Water Resour. Res.*, *9*, 1314–1323.

Jame, Y. W., and D. I. Norum (1980), Heat and mass transfer in a freezing unsaturated porous medium, *Water Resour. Res.*, *16*, 811–819.

Jansson, P.-E., and L. Karlberg (2001), Coupled heat and mass transfer model for soil-plant-atmosphere systems, *TRITAAMI Rep. 3087*, R. Inst. of Technol., Stockholm.

Jordan, R. A. (1991), One dimensional temperature model for a snow cover: Technical Documentation for SNTHERM.89, *Spec. Rep. 91-16*, Cold Reg. Res. and Eng. Lab., U.S. Army Corps of Eng., Hanover, N. H.

Koren, V., J. Schaake, K. Mitchell, Q. Y. Duan, F. Chen, and J. M. Baker (1999), A parameterization of snowpack and frozen ground intended for NCEP weather and climate models, *J. Geophys. Res.*, *104*(D16), 19,569–19,585, doi:10.1029/1999JD900232.

Kulik, V. Y. (1978), *Water Infiltration Into Soil* (in Russian), 93 pp., Gidrometeoizdat, Moscow.

Li, Q. (2008), The study of universal soil-snow cover model coupling heat and mass transport processes in land surface process, Ph.D. thesis, 167 pp., Inst. of Atmos. Phys., Chin. Acad. of Sci., Beijing.

Ling, F., and T. J. Zhang (2004), A numerical model for surface energy balance and thermal regime of the active layer and permafrost containing unfrozen water, *Cold Reg. Sci. Technol.*, *38*, 1–15.

Lunardini, V. J. (1996), Climatic warming and the degradation of warm permafrost, *Permafrost Periglacial Processes*, *7*, 311–320.

Mikan, C. J., J. P. Schimel, and A. P. Doyle (2002), Temperature controls of microbial respiration above and below freezing in arctic tundra soils, *Soil Biol. Biochem.*, *34*, 1785–1795.

Mölders, N., and J. E. Walsh (2004), Atmospheric response to soil-frost and snow in Alaska in March, *Theor. Appl. Climatol.*, *77*, 77–105.

Niu, G. Y., and Z. L. Yang (2006), Effects of frozen soil on snowmelt runoff and soil water storage at a continental scale, *J. Hydrometeorol.*, *7*, 937–952.

Pauwels, V. R. N., and E. F. Wood (1999), A soil-vegetation-atmosphere transfer scheme for the modeling of water and energy balance processes in high latitudes. Part 1: Model improvements, *J. Geophys. Res.*, *104*(D22), 27,811–27,822, doi:10.1029/1999JD900005.

Poutou, E., G. Krinner, C. Genthon, and N. de Noblet-Ducoudré (2004), Role of soil freezing in future boreal climate change, *Clim. Dyn.*, *23*, 621–639.

Richards, L. A. (1931), Capillary conduction of liquids in porous mediums, *Physics*, *1*, 318–333.

Robinson, P. J., and A. Henderson-Sellers (1999), *Contemporary Climatology*, 344 pp., Prentice-Hall, Upper Saddle River, N. J.

Romanovsky, V. E., T. E. Osterkamp, and N. S. Duxbury (1997), An evaluation of three numerical models used in simulations of the active layer and permafrost temperature regimes, *Cold Reg. Sci. Technol.*, *26*, 195–203.

Sellers, P. J., Y. Mintz, Y. C. Sud, and A. Dalcher (1986), A simple biosphere model (SIB) for use within general circulation models, *J. Atmos. Sci.*, *43*, 505–531.

Shoop, S. A., and S. R. Bigl (1997), Moisture migration during freeze and thaw of unsaturated soils: Modeling and large scale experiments, *Cold Reg. Sci. Technol.*, *25*, 33–45.

Slater, A. G., A. J. Pitman, and C. E. Desborough (1998), Simulation of freeze-thaw cycles in a general circulation model land surface scheme, *J. Geophys. Res.*, *103*(D10), 11,303–11,312, doi:10.1029/97JD03630.

Smirnova, T. G., J. M. Brown, S. G. Benjamin, and D. Kim (2000), Parameterization of cold-season processes in the MAPS land-surface scheme, *J. Geophys. Res.*, *105*(D3), 4077–4086, doi:10.1029/1999JD901047.

Spaans, E. J. A., and J. M. Baker (1996), The soil freezing characteristic: Its measurement and similarity to the soil moisture characteristic, *Soil Sci. Soc. Am. J.*, *60*, 13–19.

Sun, S., J. Jin, and Y. Xue (1999), A simple snow-atmosphere-soil transfer model, *J. Geophys. Res.*, *104*(D16), 19,587–19,597.

Sun, S., X. Zhang, and G. Wei (2003), A simplified version of the coupled heat and moisture transport model, *Global Planet. Change*, *37*, 265–276.

Takata, K., and M. Kimoto (2000), A numerical study on the impact of soil freezing on the continental-scale seasonal cycle, *J. Meteorol. Soc. Jpn.*, *78*, 199–221.

Taylor, G. S., and J. N. LUthin (1978), A mdoel for coupled ehat and moisture transfer during soil freezing, *Can. Geotech. J.*, *15*, 548–555.

Viterbo, P., A. Beljaars, J. F. Mahfouf, and J. Teixeira (1999), The representation of soil moisture freezing and its impact on the stable boundary layer, *Q. J. R. Meteorol. Soc.*, *125*, 2401–2426.

Warrach, K., H. T. Mengelkamp, and E. Raschke (2001), Treatment of frozen soil and snow cover in the land-surface model SEWAB, *Theor. Appl. Climatol.*, *70*, 23–37.

Williams, J. R. (1970), Groundwater in the permafrost regions of Alaska, *U.S. Geol. Surv. Prof. Pap.*, 696, 83 pp.

Williams, P. J. (1967), *Properties and Behaviors of Freezing Soils*, *Publ. 72*, 119 pp., Norw. Geotech. Inst., Oslo.

Xu, X. Z., J. D. Wang, and L. X. Zhang (2001), *Frozen Soil Physics*, Sci. Publ., Beijing.

Xue, Y., F. J. Zeng, and C. A. Schlosser (1996), SSiB and its sensitivity to soil properties—A case study using HAPEX-Mobilhy data, *Global Planet. Change*, *13*, 183–194.

Zhang, T., R. G. Barry, K. Knowles, J. A. Heginbottom, and J. Brown (1999), Statistics and characteristics of permafrost and ground ice distribution in the Northern Hemisphere, *Polar Geogr.*, *23*, 147–169.

Zhang, X. (2004), The study of land surface processes occurs in the arid and frozen area—Model developing, Ph.D. thesis, 210 pp., Inst. of Atmos. Phys., Chin. Acad. of Sci., Beijing.

Zhang, X., S. F. Sun, and Y. K. Xue (2007), Development and testing of a frozen soil parameterization for cold region studies, *J. Hydrometeorol.*, *8*, 690–701.

Zhao, L., and D. M. Gray (1997), A parametric expression for estimating infiltration into frozen soils, *Hydrol. Processes*, *11*, 1761–1775.

Zhao, L., D. M. Cray, and D. H. Male (1997), Numerical analysis of simultaneous heat and water transfer during infiltration into frozen ground, *J. Hydrol.*, *200*, 345–363.

Zimov, S. A., I. P. Semiletov, S. P. Daviodov, Y. V. Voropaev, S. F. Prosiannikov, C. S. Wong, and Y. H. Chan (1993), Wintertime CO_2 emission from soils of northeastern Siberia, *Arctic*, *46*, 197–204.

Q. Li, Center for Monsoon System Research, Institute of Atmospheric Physics, Chinese Academy of Sciences, P.O. BOX 2718, Beijing, 100190, China. (qian@mail.iap.ac.cn)

S. Sun, State Key Laboratory of Numerical Modeling for Atmospheric Sciences and Geophysical Fluid Dynamics, Institute of Atmospheric Physics, Chinese Academy of Sciences, P.O. BOX 9804, Beijing, 100029, China. (ssf@lasg.iap.ac.cn)

Y. Xue, Department of Geography, Department of Atmospheric and Oceanic Sciences, University of California, Los Angeles, CA 90095-1524, USA. (yxue@geog.ucla.edu)